

Aus der
Poliklinik für Zahnerhaltung und Parodontologie
Klinikum der Ludwig-Maximilians-Universität München



Digital Transformation of Dentistry through Novel Numerical and Manufacturing Approaches

Dissertation
zum Erwerb des Doctor of Philosophy (Ph.D.)
an der Medizinischen Fakultät
der Ludwig-Maximilians-Universität München

vorgelegt von
Po-Chun Tseng

aus
Taipei City / Taiwan

Jahr
2025

Mit Genehmigung der Medizinischen Fakultät der
Ludwig-Maximilians-Universität München

Erstes Gutachten: Prof. Dr. Karl-Heinz Kunzelmann
Zweites Gutachten: Priv. Doz. Dr. Andreas Kessler
Drittes Gutachten: Prof. Dr. Jürgen Manhart
Viertes Gutachten: Prof. Dr. Martin Rosentritt

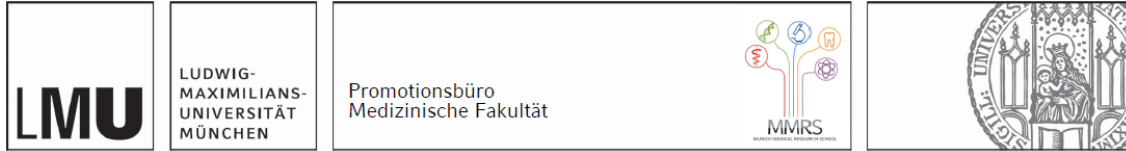
Dekan: Prof. Dr. med. Thomas Gudermann

Tag der mündlichen Prüfung: 28.05.2025

Dedicated to my family for their love and support

The work was made possible with the support of a scholarship from the German Academic Exchange Service (DAAD).

Affidavit



Affidavit

Tseng, Po-Chun
Surname, first name

Goethestraße 70
Street

80336 München, Germany
Zip code, town, country

I hereby declare, that the submitted thesis entitled:

Digital Transformation of Dentistry through Novel Numerical and Manufacturing Approaches

is my own work. I have only used the sources indicated and have not made unauthorised use of services of a third party. Where the work of others has been quoted or reproduced, the source is always given.

I further declare that the dissertation presented here has not been submitted in the same or similar form to any other institution for the purpose of obtaining an academic degree.

München, 09.06.2025
place, date

Tseng, Po-Chun
Signature doctoral candidate

Confirmation of congruency



**Confirmation of congruency between printed and electronic version of
the doctoral thesis**

Tseng, Po-Chun
Surname, first name

Goethestraße 70
Street

80336 München, Germany
Zip code, town, country

I hereby declare, that the submitted thesis entitled:

Digital Transformation of Dentistry through Novel Numerical and Manufacturing Approaches

is congruent with the printed version both in content and format.

München, 09.06.2025
place, date

Tseng, Po-Chun
Signature doctoral candidate

Table of content

Affidavit	2
Confirmation of congruency	3
Table of content	4
List of abbreviations	5
List of publications	6
1. Author’s contribution to the publications	7
1.1 Contribution to publication 1.....	7
1.2 Contribution to publication 2.....	7
1.3 Contribution to publication 3.....	7
2. Introductory summary	9
2.1 Introduction	9
2.1.1 Publication 1. Simulating the shrinkage-induced interfacial damage around Class I composite resin restorations with damage mechanics	10
2.1.2 Publication 2. Elucidating interfacial failure of cervical restorations using damage mechanics: A finite element analysis	12
2.1.3 Publication 3. Direct ink writing with dental composites: A paradigm shift toward sustainable chair-side production	13
2.2 Usage of generative AI in this dissertation	15
3. Publication 1	17
4. Publication 2	19
5. Publication 3	27
6. References	37
Curriculum vitae	40
Acknowledgements	42

List of abbreviations

AM	Additive manufacturing
CAD/CAM	Computer-aided design and computer-aided manufacturing
CZM	Cohesive zone model
DIW	Direct ink writing
FE	Finite element
FEA	Finite element analysis
LED	Light-emitting diode
LLM	Large language model
OCT	Optical coherence tomography
RMS	Root mean square

List of publications

Journal publications

Tseng P-C, Chuang S-F, Kaisarly D, Kunzelmann K-H. Simulating the shrinkage-induced interfacial damage around Class I composite resin restorations with damage mechanics. *Dent Mater* 2023;39:513–21. <https://doi.org/10.1016/j.dental.2023.03.020>.

Tseng P-C, Chuang S-F, Schulz-Kornas E, Kunzelmann K-H, Kessler A. Elucidating interfacial failure of cervical restorations using damage mechanics: A finite element analysis. *J Dent Sci* 2025. <https://doi.org/10.1016/j.jds.2024.05.033>.

Tseng P-C, Shieh D-B, Kessler A, Kaisarly D, Rösch P, Kunzelmann K-H. Direct ink writing with dental composites: A paradigm shift toward sustainable chair-side production. *Dent Mater* 2024. <https://doi.org/10.1016/j.dental.2024.08.002>.

1. Author's contribution to the publications

1.1 Contribution to publication 1

- Conceptualization: Identified knowledge gap, proposed damage mechanics incorporation in finite element modeling, developed research questions and study design (with main supervisor).
- Methodology: Created the finite element model.
- Software: Planned the experiment and prepared simulation code.
- Investigation: Collected and prepared data for analysis.
- Formal analysis: Conducted statistical analysis, produced tables and figures.
- Data Curation: Managed data in online repository.
- Writing - Original Draft: Wrote the main draft of the manuscript.
- Writing - Review & Editing: Revised the manuscript based on co-author input and directed submission to the journal.

1.2 Contribution to publication 2

- Conceptualization: Identified knowledge gap, initiated sub-project, developed research questions and study design.
- Methodology: Created the finite element model based on a public dataset.
- Software: Planned the experiment and prepared simulation code.
- Investigation: Collected and prepared data for analysis.
- Formal analysis: Conducted statistical analysis, produced tables and figures.
- Data Curation: Managed data in online repository.
- Writing - Original Draft: Wrote the main draft of the manuscript.
- Writing - Review & Editing: Revised the manuscript based on co-author input and directed submission to the journal.

1.3 Contribution to publication 3

- Conceptualization: Developed research questions and study design (with main supervisor).
- Methodology: Established printing calibration workflow and planned the experiment.
- Software: Prepared script for automated deviation quantification.

- Investigation: Performed the experiment, collected and prepared data for analysis.
- Formal analysis: Conducted statistical analysis, produced tables and figures.
- Writing - Original Draft: Wrote the main draft of the manuscript.
- Writing - Review & Editing: Extensively revised the manuscript based on co-author input and directed submission to the journal.

2. Introductory summary

Name of the project: Digital Transformation of Dentistry through Novel Numerical and Manufacturing Approaches

This dissertation presents the results of the research projects conducted at the Department of Conservative Dentistry and Periodontology, University Hospital, Ludwig Maximilian University, Munich, under the supervision of Prof. Dr. Karl-Heinz Kunzelmann, PD. Dr. Andreas Kessler, Prof. Dr. Peter Rösch, PD. Dr. Dalia Kaisarly.

The project investigated the interfacial damage of dental composite resin restorations using finite element analysis and explored the potential of a novel extrusion-based 3D printing system for dental applications. The findings are presented in three peer-reviewed publications.

2.1 Introduction

While composite resin restorations offer a reliable solution to restore smaller tooth defects, achieving optimal results for larger restorations remains challenging. The shrinkage during the polymerization process generates stress that can damage the bonding interface, potentially leading to debonding and secondary caries [1]. Additionally, reconstructing large defects intraorally by hand requires significant technical and also artistic expertise [2,3]. To address these limitations and achieve predictable, cost-effective definitive restorations, this dissertation focuses on two key aspects: 1) utilizing advanced in silico modeling methods to improve our understanding of the debonding phenomenon, and 2) developing a novel manufacturing approach for producing high-quality, affordable indirect restorations.

Finite element (FE) methods allow us to model mechanical stress and strain based on physical principles, providing valuable biomechanical insights for clinical practice. However, previous FE studies often assumed a perfect bond between the modeled parts [4–6]. This limitation hinders their ability to capture the highly non-linear process of interfacial damage and debonding [7,8]. Since debonding may lead to unfavorable outcomes including hypersensitivity and secondary caries, incorporating damage mechanics into FE models is crucial for more realistic and clinically relevant analyses.

While numerical modeling helps us understand the stresses and damage around restorations, limitations persist in how these restorations are produced. Larger defects of

tooth structure are better restored using indirect restorations for reduced shrinkage stress and more precise control of occlusion and morphology [9]. Being extraorally fabricated by dental technicians in the past, these indirect restorations offer more predictable outcomes compared to direct restorations formed by dentists' intraoral freehand shaping. However, the traditional manual fabrication of indirect restorations is time-consuming and labor-intensive, leading to high costs and hindering the affordability of the indirect restorations. In this context, I investigated a novel manufacturing approach for indirect restorations in the last publication.

The development of chairside computer-aided design and computer-aided manufacturing (CAD/CAM) systems has revolutionized the production of indirect restorations. While subtractive CAM systems offer significant advantages by enabling faster turnaround times compared to traditional laborious methods, affordability remains a key barrier to their widespread adoption [10]. The high costs of milling machines and material blocks associated with subtractive CAD/CAM pose a significant challenge. Furthermore, the subtractive nature of this manufacturing process always leads to significant material waste and tool wear [10,11]. These limitations have fostered the ongoing development of alternative manufacturing processes that aim to achieve greater affordability and reduced waste generation.

This dissertation addresses the limitations discussed above through three peer-reviewed journal articles. The first two journal articles investigate how shrinkage stress and occlusal loads affect the development of interfacial damage around dental restorations, using damage mechanics-based FE modeling. The last publication presents a novel extrusion-based 3D printing system specifically designed for clinically approved dental resin composites. This system offers enhanced affordability while using materials with desired mechanical properties for permanent restorations. Further details regarding the methodology and findings of these publications are provided in the following sections.

2.1.1 Publication 1. Simulating the shrinkage-induced interfacial damage around Class I composite resin restorations with damage mechanics

This study introduces a cohesive zone model (CZM) to investigate the effects of shrinkage on interfacial damage in Class I composite resin restorations. Recognizing the necessity of incorporating damage mechanics into FE analysis, the CZM defines the interfacial stiffness at the composite-tooth junction based on published interfacial properties, including critical stress and fracture energy (also referred to as critical ener-

gy release rate). This allows the bonding interface to exhibit damage behavior, demonstrating a reduced interfacial stiffness after reaching the defined critical stress [7]. Upon dissipating the fracture energy, the interface becomes completely debonded and no longer withstands any further stress.

A simplified geometry was designed to represent the dimensions of the tooth structure and a Class I cavity (defect) filled with dental composites. Shrinkage of the composite part was simulated using a temperature drop analogous to thermal shrinkage [12]. The size of the cavity was systematically varied to investigate the extent of damage surrounding cavities of different sizes. The size variation was the reason why a Class I cavity was chosen. Contraction during polymerization in a Class I cavity induces hoop stress, which at best leads to elastic deformation of the tooth structure under the stresses that can arise from composite polymerization. However, this deformation is much smaller compared to the cusp deformation in Class II defects and can be largely neglected for our model. In Class II cavities, cusp compliance would have a non-trivially predictable influence on the interfacial stresses, whereby both the remaining cusp thickness and cavity heights are included as parameters in the cusp compliance. The Class I cavity is therefore a more standardized approach to investigate the effects at the interface depending on the cavity geometry.

To understand how damage affects the stress distribution around the restoration, a conventional FE model assuming a perfect bond was also created for the case with a restoration of 2-millimeter height and diameter. Maximum principal stress was plotted along the bonding interface for both the CZM and perfect-bond models. Additionally, the displacement fields were visualized to compare the shrinkage patterns [13,14].

The results showed that interfacial damage was initiated at the occlusal margin and internal line angles of the bonding interface. By comparing the stress distribution between the CZM and perfect-bond models, I found that interfacial damage led to stress relief near the center of the damaged area and elevated stress at the tips of the damage. Due to the loss of adhesion to the tooth in the defect area, the material, which has been stretched by contraction with intact adhesion, relaxes, making local shrinkage more prominent near the damaged interface in the CZM compared to that of the perfect-bond model.

Finally, the extent of interfacial damage differed among CZM models with varying restoration dimensions. In general, more confined restorations with smaller diameters and greater depths experienced more severe interfacial damage. This finding agrees in principle with the well-known C-factor theory (the ratio of bonded area to unbonded surface area). Previous C-factor theory suggests that restorations with a higher C-

factor are more susceptible to debonding due to greater shrinkage stress [15–17]. However, our study also revealed that the relationship between the extent of damage and the C-factor was not always straightforward. This finding highlights the need for additional refinement of the C-factor concept for a more accurate assessment of debonding risk [18,19].

2.1.2 Publication 2. Elucidating interfacial failure of cervical restorations using damage mechanics: A finite element analysis

To extend the application of the CZM in clinical scenarios, I simulated interfacial damage of cervical composite restorations in the second publication, aiming to illustrate the role of compressive occlusal loads in interfacial debonding. Given the association between occlusal wear facets and debonding of cervical restorations, parafunction and excessive excursive jaw movements have been hypothesized to be major threats to the bond integrity [20]. However, the damage process has not been demonstrated in in vitro laboratory experiments or through computer simulations. Although there are FE studies showing that occlusal loads with horizontal components (toward buccal or lingual direction) result in greater interfacial stress around cervical restorations [21,22], conventional FE models cannot illustrate the extent and implications of damage without considering damage mechanics.

In this study, I utilize the CZM to analyze interfacial damage around cervical restorations. An anatomical plane-strain model was created based on a micro-computed tomography image of an upper premolar [23]. Gradually increasing compressive loads (from 0 to 150 N) were applied at the midpoints of the occlusal slopes in three distinct modes: an oblique (45 degrees to the long axis of the tooth) load at the buccal triangular ridge, an oblique load at the palatal triangular ridge, and two equal-magnitude axial (parallel to the long axis of the tooth) loads applied at both ridges.

The results indicate that the axial compressive loads exert a less detrimental effect on the bonding interface, with damage initiating at a combined load of 260 N. In contrast, the oblique loading modes initiated interfacial damage at lower forces: 100 N for buccal oblique and 120 N for palatal oblique loading. The damage, similar to defects that cause stress concentration, led to greater stress at the adjacent interface. Furthermore, comparisons of the stress distributions between the perfect-bond models and their respective CZM models revealed an unexpected change in stress patterns at a distant site. Specifically, under a buccal oblique compressive load of 150 N, a 23% increase (42 MPa) in the maximum principal stress was observed in the CZM model at the occlusal groove, posing a potential threat to the structural integrity at that location.

The study demonstrates that occlusal loads can indeed lead to the debonding of cervical restorations and identified occlusal load direction as a key determinant of their bond integrity. The results thus underline the necessity to assess occlusal factors before restoring cervical defects. It is worth noting that this study only assessed three specific scenarios of compressive loads. A force can be fully characterized by its point of application and the properties (directions and magnitudes) of its decomposed components. Building on this understanding, further research could systematically vary the point of application and vector components to dissect their respective effects.

The two FE studies were both conducted using Salome-MECA, an open-source computer-aided engineering and numerical simulation platform [24,25]. In accordance with the principles of open science, the mesh, code, and results have been archived and made publicly available on an online repository (<https://doi.org/10.17605/OSF.IO/926KT> and <https://doi.org/10.17605/OSF.IO/84ZGY>). This commitment to open science fosters reproducibility and facilitates collaboration within the research community.

2.1.3 Publication 3. Direct ink writing with dental composites: A paradigm shift toward sustainable chair-side production

Compared to subtractive manufacturing techniques, additive manufacturing can achieve more affordable production with reduced machine costs [10]. Additive manufacturing principles have been applied in the production of both ceramic and resin-based composite restorations. While additively manufactured ceramic restorations have demonstrated good mechanical strength and dimensional accuracy, their fabrication process still requires specialized equipment for post-processing, necessitating additional investments. Furthermore, the prolonged high-temperature post-processing treatment (debinding and sintering) hinders on-demand production and renders chair-side application unrealistic [26]. These disadvantages make additively manufactured ceramic restorations impractical for most clinical practices.

With respect to additive manufacturing of resin-based restorations, most research and innovations have been developed based on the vat-photopolymerization principle. The vat-photopolymerization systems are incompatible with high-viscosity materials because highly viscous materials can impede material inflow during the printing process, which may lead to defects and dimensional inaccuracies in the final product [27,28]. However, modern high-performance dental composites typically contain viscous resin monomers and a large proportion of sub-micro-sized inorganic fillers to achieve adequate mechanical properties and wear resistance [29]. Due to their composition, these

high-performance composites are too viscous for the vat-photopolymerization process. Thus, manufacturers often compromise on the composition of resin-based materials to reduce their viscosity for vat-photopolymerization systems, sacrificing the physical properties of the printed products. Consequently, composite restorations produced by additive manufacturing systems currently in the dental market are better suited for interim usage rather than definitive treatments [30].

To overcome these limitations, a new 3D printing system based on the extrusion-based direct ink writing (DIW) principle was developed at the LMU dental clinic. The DIW technique can work with materials with 100 times the viscosity of those used in the vat-photopolymerization systems (10^3 Pa·s versus 10 Pa·s) [28,31]. This feature enables the use of resin composites with high filler contents and ensures the ideal physical properties of the printed restorations. With a primary goal of clinical application, our system utilizes a clinically approved flowable composite for printing. The composite can achieve adequate mechanical properties and wear resistance, promoting predictable long-term clinical success.

The system is equipped with tunable light-emitting diodes (LEDs) for controlled photopolymerization to reduce material slumping [32], where the extruded viscoplastic material collapses due to its own weight and compromises the dimensional accuracy of the printed object [33]. By applying a low-dose light curing regime during the extrusion process, the composite reached the gel point shortly after being extruded so that the material could no longer flow or collapse. Accordingly, the printing accuracy was substantially improved without clogging the nozzle. Furthermore, the extrusion flow rate and scaling factors were optimized through printing and characterization of basic geometries, including straight lines and cylinders. These optimizations ensure consistent material deposition and accurate dimensional control for fabricating dental restorations.

To examine the feasibility of the novel DIW approach for dental applications, I printed multiple occlusal veneers ($n = 20$) and evaluated their dimensional accuracy. The printed samples were scanned with a high-resolution confocal 3D scanner and then compared with the original CAD model (reference surface) to assess how accurately the printed restorations reproduce the original design. Specifically, the scans of the surface were first finely registered to the reference using an iterative closest point (ICP) algorithm. Then, cloud-to-cloud (C2C) distances were computed to quantify the deviations from the reference for every surface point on the samples. Furthermore, to assess the precision of the printing process, the surface scans of the occlusal veneers were compared with each other. The ICP alignment process and C2C distance computations were conducted using the open-source software CloudCompare.

The quantitative analysis indicated good dimensional accuracy, with a sample-specific trueness (deviation of each sample surface from the reference CAD model) of $30.1 \pm 1.9 \mu\text{m}$ and a pair-specific precision (deviations of printed veneers) of $26.7 \pm 4.5 \mu\text{m}$ (mean \pm standard deviation). Furthermore, the deviation maps revealed several isolated areas with higher deviations ($> 100 \mu\text{m}$) in the form of protuberant excess.

To identify the cause of these areas of high deviation, I conducted a thorough inspection of the printing process on the level of the g-code, which is used to control the printer. Since our DIW printer was built based on the 3-axis (x/y/z) kinematics, the object was sliced perpendicular to the vertical z-axis for layer-by-layer printing. As a result, when there is more than one enclosed area to be printed within a single layer, the extruder must travel without extruding material (non-extrusion movements) to move from one to the next printing area. These non-extrusion travel paths can lead to printing inaccuracy by causing material stringing, where excess material is dragged out from the printed regions like thin threads, or oozing, where the material is extruded unintentionally during travel [34]. In the case of the occlusal veneer for a posterior tooth, the presence of multiple cusps inevitably results in separate areas to be filled in a single z-slice. Accordingly, the non-extrusion travel across the valleys (occlusal fissures) constitutes a potential source of dimensional deviation.

To visualize the effects of the non-extrusion movements, I extracted the non-extrusion paths from g-code and overlaid them on the deviation map. This analysis revealed that the areas with the highest deviations coincided with the non-extrusion perimeter-crossing sites (locations where the extruder moved across the already printed outer walls to the next printing region). The finding suggests that material stringing is the main cause of these protuberant inaccuracies.

This study highlights the potential of the DIW 3D printing system for restorative dentistry, demonstrating clinically relevant dimensional accuracy. Future efforts should be directed towards utilizing DIW printing for dental composites with even higher filler content, developing novel printing strategies to minimize material stringing, and exploring multi-material printing capabilities.

2.2 Usage of generative AI in this dissertation

The initial draft of this introductory summary was formed independently by Po-Chun Tseng without using any generative AI tool. Afterward, the draft was refined by a large language model (LLM) named Gemini, developed by Google DeepMind. The LLM's output was thoroughly reviewed sentence-by-sentence by Po-Chun Tseng and selec-

tively incorporated to improve the language flow for better scientific communication. This cautious usage ensured correctness and rigor while enhancing the clarity of the text.

The dialogue thread with the LLM and the initial draft, prompts, and LLM outputs have all been archived in an online repository (<https://doi.org/10.17605/OSF.IO/EGWYU>) for further reference. The roles of LLMs in the second and third manuscripts are also specified in the attached publications.

3. Publication 1

Simulating the shrinkage-induced interfacial damage around Class I composite resin restorations with damage mechanics

Po-Chun Tseng, Shu-Fen Chuang, Dalia Kaisarly, Karl-Heinz Kunzelmann

Dent Mater 2023;39:513–21.

<https://doi.org/10.1016/j.dental.2023.03.020>.

Accepted manuscript in the preprint server (OSF Preprints):

<https://doi.org/10.31219/osf.io/e56dm>

The formatted publication is not included due to copyright agreements. Please access <https://doi.org/10.1016/j.dental.2023.03.020> (publication behind a paywall) or alternatively <https://doi.org/10.31219/osf.io/e56dm> (open access accepted manuscript).

4. Publication 2

Elucidating interfacial failure of cervical restorations using damage mechanics: A finite element analysis

Po-Chun Tseng, Shu-Fen Chuang, Ellen Schulz-Kornas,
Karl-Heinz Kunzelmann, Andreas Kessler

J Dent Sci 2025;20:410–6.

<https://doi.org/10.1016/j.jds.2024.05.033>.

Available online at www.sciencedirect.com

ScienceDirect

journal homepage: www.e-jds.com

Original Article

Elucidating interfacial failure of cervical restorations using damage mechanics: A finite element analysis

Po-Chun Tseng ^{a*}, Shu-Fen Chuang ^{b,c}, Ellen Schulz-Kornas ^d,
Karl-Heinz Kunzelmann ^a, Andreas Kessler ^{a,e}

^a Department of Conservative Dentistry and Periodontology, University Hospital, LMU Munich, Munich, Germany

^b School of Dentistry and Institute of Oral Medicine, College of Medicine, National Cheng Kung University, Tainan, Taiwan

^c Department of Stomatology, National Cheng Kung University Hospital, Tainan, Taiwan

^d Department of Cariology, Endodontology and Periodontology, University of Leipzig, Leipzig, Germany

^e Department of Prosthetic Dentistry, Faculty of Medicine, Center for Dental Medicine, Medical Center-University of Freiburg, Freiburg, Germany

Received 16 May 2024; Final revision received 29 May 2024

Available online 12 June 2024

KEYWORDS

Debonding;
Dental restorations;
Finite element
analysis

Abstract *Background/purpose:* Although clinical studies have suggested a link between non-axial forces and reduced longevity of cervical restorations, the underlying mechanisms require further numerical investigation. This in-silico study employed a cohesive zone model (CZM) to investigate interfacial damage in a cervical restoration subjected to different load directions. *Materials and methods:* A plane strain model of a maxillary premolar was established, with a wedge-shaped buccal cervical restoration. To simulate debonding, the restoration-tooth interface was modeled by the CZM, which defines the strain-softening damage behavior based on interfacial stress and fracture energy. Occlusal loads were applied in three different directions: (1) obliquely on the buccal triangular ridge, (2) obliquely on the palatal triangular ridge, and (3) equal magnitude axially on both ridges. Damage initiation and progression were analyzed, and stress distribution in damaged models was compared with the corresponding perfect-bond models.

Results: Non-axial oblique loads initiated damage at lower forces (100 N for buccal and 120 N for palatal) compared to axial loads (130 N on both ridges). After debonding, buccal oblique loading caused higher stress at the central groove (42.5 MPa at 150 N). Furthermore, buccal oblique loading resulted in more extensive debonding than that caused by the palatal oblique load (88.3% vs. 43.3% of the bonding interface at 150 N).

* Corresponding author. Department of Conservative Dentistry and Periodontology, University Hospital, LMU Munich, Goethestr. 70, Munich 80336, Germany.

E-mail address: P.Tseng@campus.lmu.de (P.-C. Tseng).

<https://doi.org/10.1016/j.jds.2024.05.033>

1991-7902/© 2025 Association for Dental Sciences of the Republic of China. Publishing services by Elsevier B.V. This is an open access article under the CC BY license (<http://creativecommons.org/licenses/by/4.0/>).

Conclusion: The study provides numerical evidence supporting the tooth flexure hypothesis, that non-axial forces are more detrimental to the bonding interface of the cervical restoration. The results highlight the necessity of damage mechanics in deriving stress distribution upon debonding.

© 2025 Association for Dental Sciences of the Republic of China. Publishing services by Elsevier B.V. This is an open access article under the CC BY license (<http://creativecommons.org/licenses/by/4.0/>).

Introduction

In the absence of dental caries, chronic loss of cervical tooth tissue may still occur due to wear, erosion, and abfraction.¹ The resulting lesions are often referred to as noncarious cervical lesions (NCCLs). A cross-sectional study has reported that 67.8% of patients admitted to a dental school clinic had at least one NCCL lesion.² If left unrepaired, the lesions are prone to progress with age, posing a threat to pulp vitality and structural integrity of the affected teeth.¹

Despite the importance of cervical restorations in arresting NCCL progression, achieving long-lasting retention and interfacial integrity remains a challenge in clinical practice. Compromised bond integrity can lead to negative consequences, such as hypersensitivity and secondary caries.³ On average, 24% of the cervical restorations may exhibit marginal discoloration and 10% would be lost within 3 years.⁴

Occlusal stress has been recognized as a key contributing factor to NCCLs. Clinical studies have shown correlations between parafunctional habits, wear facets, and the presence of NCCLs, suggesting that excessive occlusal loads contribute to the development of these cervical defects.^{5,6} Likewise, cervical restorations are at a higher risk of debonding in teeth with wear facets.³ Since non-axial occlusal loads can be transferred through the crown and create concentrated stress in the cervical region of the tooth, the non-axial loads and the resulting tooth flexure are hypothesized to be a primary cause of interfacial failures observed around cervical restorations.^{7,8}

Finite element analysis (FEA) has been utilized extensively in in-silico dental biomechanics to model clinically relevant scenarios.^{9–11} Despite the difficulty to model local variations in material properties, previous FEA still provided valuable insights into the impact of occlusal loads on cervical restorations, demonstrating that non-axial forces are associated with higher tensile stress at the bonding interface.^{8,10} However, a key limitation of conventional FEA models is the assumption of a perfect bond at the restoration-tooth interface. This assumption prevents them from capturing the process of bond deterioration and limits their validity to the point of interfacial damage initiation.

To overcome the limitations of the conventional FEA, damage mechanics must be incorporated to properly model interfacial debonding. In this study, we simulate the interfacial damage using a cohesive zone model (CZM) to derive the extent of damage and its consequences. Originally developed to simulate the crack for brittle fracture, the CZM has been successfully adapted to model debonding

in adhesive joints, including the restoration-tooth interfaces.^{12,13} For comparison, we also build FEA models assuming perfect bonding at the interface. This allows us to directly assess the influence of interfacial damage on stress distribution.¹⁴

The null hypotheses tested in this study were: (1) The extent of interfacial damage would not differ due to variations in occlusal force direction. (2) The presence of interfacial damage had no effect on the maximum principal stress distribution.

Materials and methods

Geometry and mesh

A 2D plane strain model of a maxillary human premolar was built based on a sagittal slice of a micro-CT scan.¹⁵ A wedge-shaped composite restoration for an artificial NCCL, consisting of an equilateral triangle with a 1.85 mm base and a 0.3 mm fillet at the apex, was incorporated at the buccal cervical region. The surrounding periodontal structures, including the periodontal ligament, cortical bone, and trabecular bone, were included to better represent the clinical scenario. The structures were meshed with first-order triangular elements using the Netgen algorithm (Fig. 1a). The global mesh size ranged between 0.25 and 0.0025 mm, with a finer mesh employed in critical areas: 0.1 mm for the periodontal ligament, 0.125 mm for the composite restoration, and a refined element size of 0.025 mm along the bonding interface.

Mesh convergence was evaluated with respect to the greatest maximum principal stress value and the damaged proportion of the bonding interface. By conducting computations on meshes with increasing density, convergence was ensured since both metrics converged within a 1% tolerance.

Numerical simulation

The analysis was conducted using the open-source Salome-Meca suite (v2023 W64, EDF, Paris, France).¹⁶ In this study, the composite and the dental components were modeled as homogeneous and isotropically elastic materials. Except for the enamel-composite and dentin-composite interfaces, all interfacial connections between the tooth and supporting structures were modeled as perfectly bonded.

To simulate the debonding phenomenon at the restoration-tooth interface, a damage mechanics-based cohesive zone model (CZM) was employed. This CZM

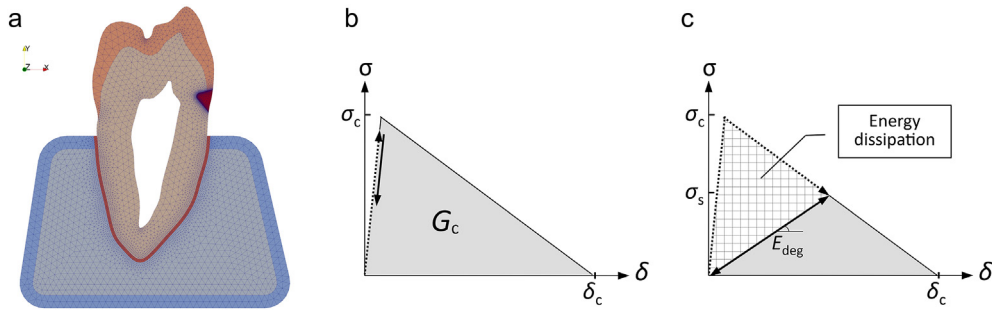


Figure 1 Meshed geometry and the strain-softening behavior defined by the cohesive zone model (CZM). (a) Meshed geometry of the tooth-PDL-bone structure with a simplified wedge-shaped restoration inserted at the buccal cervical region. (b) The CZM traction-separation curve defining the damage behavior of the interface by the interfacial stress (σ) and separation (δ). Critical stress (σ_c) indicates the maximum permissible stress for the interface. (c) Upon reaching the critical stress, interfacial elements become damaged and demonstrate strain-softening behavior (with a reduced interfacial stiffness E_{deg}). Once energy dissipation (hatched area) reaches the critical energy release rate G_c , the element fractures and no longer bears the stress.

utilizes a bilinear traction-separation law, as illustrated in Fig. 1b. The bilinear CZM law was chosen to model the mixed-mode brittle fracture during debonding.^{13,14,17} When the interfacial elements experience stress exceeding a critical value, they exhibit strain softening damage, as the microcrack forming process observed during debonding Fig. 1c.^{18,19} The interfacial element completely debonds after dissipating the specified fracture energy. The input material and interface property values are listed in Table 1.

The finite element solver performed nonlinear quasi-static simulation using a semi-automatic timestepping algorithm. As a simplified approximation of masticatory strokes, nodal occlusal loads were applied incrementally from 0 N to 150 N in three distinct directions: (1) 45° oblique to the long axis on the buccal triangular ridge (incurive phase I), (2) 45° oblique to the long axis on the palatal triangular ridge (excursive phase II), and (3) two equal-magnitude axial forces applied on both the buccal and palatal triangular ridges (maximum intercuspation).⁶ The bottom of the cortical bone was constrained in all directions.

To illustrate the effect of debonding on stress distribution, additional FEA models were created analogous to the

conventional perfect-bond model. In these models, the interface was assigned exceptionally high critical stress and initial stiffness values (1000 times the value used in the damage mechanics model), essentially preventing debonding throughout the simulation.

Data analysis

During the post-processing stage of the simulation, the maximum principal stress was derived as an indicator of potential semi-brittle fracture initiation.²⁰ Results were visualized using the Paravis module within the Salome-Meca suite. The extent of the damaged interface was extracted and then visualized using R (version 4.1.2) and the ggplot2 package (version 3.3.5). To assess the influence of debonding, the stress difference maps were generated by subtracting the stress distribution of the perfect-bond models from that of the corresponding CZM models. Finally, to facilitate further application of the damage mechanics in dental FEA, the data and code were deposited in an open-access online repository (<https://doi.org/10.17605/OSF.IO/84ZGY>).

Results

Damage initiation and progression

An oblique load of only 100 N applied to the buccal ridge can induce extensive damage (Fig. 2, line plots illustrating the relationship between the applied load magnitude and the damage). In addition, palatal oblique loading results in less interfacial damage compared to buccal oblique loading. Table 2 further details the damage initiation force and the ultimate damage length at 150 N. The results indicate that the bonding interface is more resistant to axial loads compared to oblique loading scenarios.

Damage distribution at 150 N

Fig. 3 illustrates the spatial distribution of interfacial damage along with the corresponding maximum principal stress distribution for the three loading scenarios at 150 N.

Table 1 Properties of the material and the interface.

Components	Poisson's ratio	Elastic modulus [MPa]
Enamel, ^{26,32,a}	0.30	84,100
Dentin ^{26,32}	0.30	18,600
Composite ³³	0.35	12,000
Periodontal ligament ¹⁰	0.45	68.9
Cortical bone ¹⁰	0.30	13,700
Trabecular bone ¹⁰	0.30	1370
Interface	Critical stress [MPa]	Critical energy release rate [mJ/mm ²]
Enamel-composite ^{34,35}	34.5	0.05
Dentin-composite ^{36–38}	17.0	0.01

^a Based on the literature listed in references.

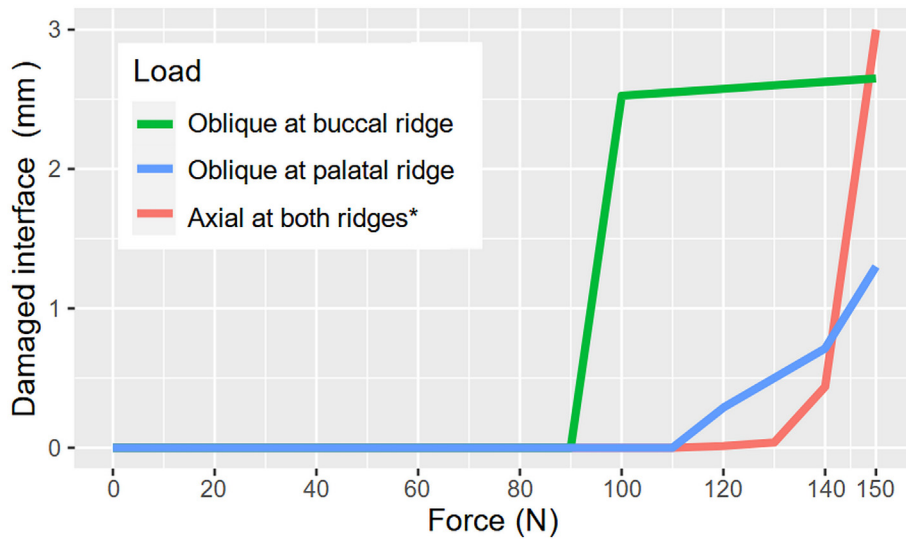


Figure 2 Line plot of damage progression under the three loading regimes, plotted against the corresponding magnitudes of the applied loads on the x-axis. For the axial loading case, two equal-magnitude forces were applied on both ridges, resulting in a total axial force twice the value indicated on the x-axis. Therefore, the line plots indicate that the bonding interface is more resistant to the axial loads.

Table 2 Force magnitude at damage initiation and the proportion of the damaged interface at 150 N.

Loading regime	Damage initiation force [N]	Damaged proportion at 150 N [%]
Buccal oblique	100	88.3
Palatal oblique	120	43.3
Axial at both ridges	130	100

*For axial loading, two equal-magnitude loads were applied on both ridges. Therefore, the tooth received twice the axial force as indicated in the table.

The results reveal extensive damage (88.3%) under buccal oblique loading, with complete debonding of the restoration-dentin interface and partial debonding of the restoration-enamel bond. In contrast, the palatal oblique load of 150 N resulted in more limited damage, affecting

only 43.3% of the bonding interface near the cavity apex. Axial loading caused complete debonding at the maximum applied load (more specifically, 150 N on both buccal and palatal triangular ridges), but it is worth noting that the interface can well withstand axial loads up to 120 N on both ridges without any damage.

Implications of damage

Fig. 4 illustrates the difference in maximum principal stress between the CZM damage models and their corresponding perfect-bond models. Positive values indicate regions where the CZM models experience higher stress compared to the perfect-bond scenarios. The presence of interfacial damage, as indicated by the hollow triangle (\triangle), leads to localized stress relief around the center of the damaged zones. However, it also induces stress concentrations at the advancing fronts of the damage (asterisks). Notably, under buccal loading, the damage model exhibits a particularly

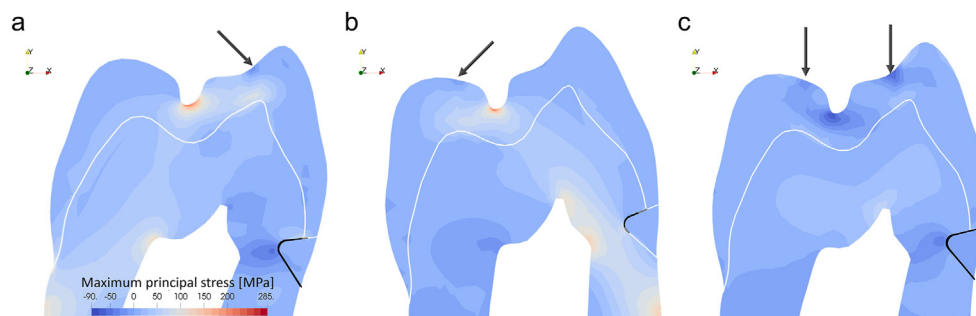


Figure 3 Maximum principal stress and interfacial damage at 150 N. Interfacial damage (black) was revealed in the deformed shapes (scale factor of 3) for better visualization. The arrows indicate the direction of the applied forces. (a) Under buccal loading, only a portion of the enamel-composite interface remains bonded. (b) In contrast, most of the interface was intact under the palatal load. (c) The interface was completely debonded when subjected to a combined axial load of 150 N on both ridges. However, it is important to note that the damage was not initiated until 130 N axial loads on both ridges.

substantial increase in stress, reaching 42.5 MPa at the central groove (Fig. 4a, ▼). These observations indicate that interfacial damage can alter stress distribution at both local and distant areas within the restoration-tooth complex.

Discussion

This study employed the CZM to investigate the complex, non-linear interfacial damage process around cervical restorations. The results demonstrate that the restoration-tooth interface exhibits greater resistance to axial loading compared to non-axial loading scenarios. These findings support the concept of tooth flexure as a key contributing factor to the debonding of cervical restorations, providing the first numerical evidence using a damage mechanics approach. Furthermore, the analysis revealed that interfacial damage alters the overall stress distribution within the restoration-tooth structure. This observation highlights the importance of incorporating damage mechanics approaches for a more comprehensive understanding of clinical scenarios involving debonding. Based on these results, the two null hypotheses are rejected, indicating that interfacial damage varies with occlusal force direction and alters stress distribution at the occlusal surface.

Considering the observed influence of interfacial damage on stress distribution, this study offers valuable insights for the management of NCCLs and provides further evidence for existing concepts. Before receiving cervical restorations, patients with occlusal wear facets or tooth malalignment should undergo a thorough evaluation of occlusal contacts, particularly during eccentric movements to identify premature contacts.^{1,2} Early restoration failure may suggest the need for re-examining occlusal contacts and reducing non-axial loading on the affected tooth. This highlights the importance of minimizing excessive non-axial forces, also a well-recognized risk factor for NCCLs.² Patients with parafunctional habits, such as bruxism, might require additional considerations. In certain scenarios, occlusal adjustments or the use of occlusal splints could be beneficial. The study also found a correlation between interfacial damage and increased stress at the occlusal groove, amplifying the existing stress concentration at the grooves of intact teeth during mastication.⁹ This may

elevate the risk of tooth fracture, similar to what is observed in cases of unrestored cervical defects.^{21,22} By incorporating interfacial damage mechanics into the FEA framework, this study represents a significant step toward achieving more clinically relevant simulations.

While clinical studies offer the most applicable information for clinical practice, their results are usually confounded by various clinician-, patient-, and even defect-dependent factors. Therefore, it is challenging to obtain mechanistic insights directly from the clinical studies. On the other hand, laboratory studies provide a well-controlled approach to isolate the effects of specific variables. However, since each tooth is unique and can only be tested once, researchers can only strive to standardize experimental procedures as much as possible. Accordingly, a complex interplay among variations and other uncertainties is inevitable, posing a challenge to dissect the contribution of each variable under investigation.

FEA offers a valuable tool to illustrate mechanical phenomena. By leveraging established physical principles, FEA can resolve the uncertainties introduced by anatomical variations and technical differences. Even though FEA can systematically delineate the effects of different variables, conventional FEA models often rely on the assumption of a perfect bond between the restoration and the tooth. This assumption limits their ability to model and predict the process of clinical bond deterioration, a crucial factor in the longevity of restorations. Furthermore, FEA based on the perfect bond assumption may derive unrealistic stress at the interface under physiological loading.

To address the limitation of the perfect-bond models, various techniques have been explored to approach debonding phenomena. The element deletion method, where interfacial connectivity is severed upon exceeding a predefined maximum stress threshold, constitutes the earliest attempt. However, this approach suffers from mesh dependency as it gives no consideration for energy dissipation.²³ Alternatively, linear elastic fracture mechanics (LEFM) has also been employed to simulate crack propagation.^{24,25} However, this method requires computationally expensive step-wise remeshing, and it is not specifically designed for interfacial debonding scenarios.¹³ Another approach involves introducing predefined non-bonded interfaces within the model.^{11,26} The static approach avoids

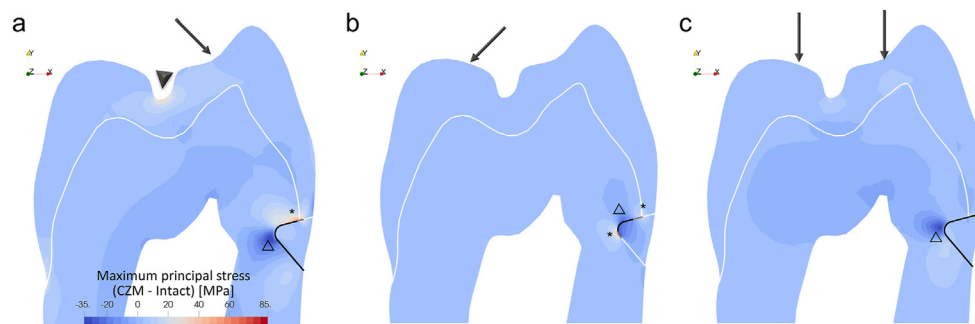


Figure 4 Difference maps of maximum principal stress distribution illustrating the effects of interfacial damage. Positive values indicate regions where the damaged models experience higher stress compared to the perfect-bond model under the same loading condition. The presence of damage leads to local stress relief (Δ) but also stress concentrations at the damage front (*). Furthermore, the figure highlights a region of increased stress (\blacktriangledown) at the central groove in the buccally loaded damaged model.

the complexities of simulating damage progression but cannot capture the progressive nature of debonding, potentially leading to significant deviations from real-world clinical situations.¹⁴ These limitations highlight the need for more rigorous models that can incorporate damage mechanics and realistically represent the initiation and propagation of interfacial debonding.

By introducing the CZM into dental FEA, our study opens a new avenue to rigorously model interfacial debonding, a crucial yet under-investigated clinical phenomenon. Unlike conventional static FEA, the CZM leverages damage mechanics principles to model the progression of debonding. This approach can also solve the intractable mesh dependency issue associated with the element deletion method. Furthermore, the CZM offers an additional advantage in terms of computational efficiency by eliminating the need for resource-intensive remeshing, which is required by the LEFM approach.

The damage distribution patterns in this study correlate well with in-vitro and clinical observations reported in the literature, highlighting the clinical relevance of our results. Nowadays, internal defects at the bonding interface can be revealed using optical coherence tomography (OCT),²⁷ allowing non-invasive imaging for damage monitoring.²⁸ After clinical service of 36–48 months, OCT has revealed a high proportion of defective restoration margin, with median values ranging from 47.9% to 92.8% depending on adhesive strategies employed.²⁹ Besides, a clear link has been established between increased interfacial defect and retention loss.³⁰ Thus, these findings strongly support the necessity of incorporating damage mechanics approaches into in-silico simulations.

The present study demonstrated the feasibility and value of CZM in modeling interfacial damage around NCCLs. As the first proof of concept, there are still aspects to be addressed to further refine and validate the novel approach. First, the model was built according to the plane strain condition, limiting the results to the mid-sagittal section. Extending the model into 3D would provide a more comprehensive picture of damage and stress distribution within the restoration-tooth complex. Second, further investigations are warranted to elucidate the extent of interfacial damage under polymerization shrinkage.³¹ Incorporating variations in relevant parameters such as the mechanical properties of restorative materials and cavity configurations would provide further insights for clinical guidance. Third, in-vitro experiments would be highly valuable to validate the model's predictions. Such experiments will need to consider anatomical variations and other potential uncertainties, but it would be advantageous to include material inhomogeneity for more accurate results via the use of realistic samples. Finally, the load directions could be systematically varied in future studies to further illustrate the relationship between load directions and interfacial damage.

In conclusion, this study represents a significant step towards achieving more clinically relevant FEA through the application of damage mechanics. The in-silico analysis provides numerical evidence for the tooth flexure hypothesis, demonstrating that non-axial forces are more detrimental to the cervical restoration's bonding interface. The analysis also reveals a crucial link between extensive

interfacial damage and increased stress at the occlusal groove, putting the integrity of the tooth structure at a higher risk. To minimize detrimental debonding and ensure the longevity of cervical restorations, careful occlusal evaluation and proper management of non-axial occlusal forces are recommended before restoring NCCLs.

Declaration of Generative AI and AI-assisted technologies in the writing process

Statement: During the preparation of this work the authors used Gemini, an artificial intelligence (AI) language model developed by Google, to improve the language of this manuscript. After using this service, the authors reviewed and edited the content as needed and take full responsibility for the content of the publication.

Declaration of competing interest

The authors have no conflicts of interest relevant to this article.

Acknowledgments

The authors would like to thank Prof. Dr. Peter Rösch and Mr. Thomas Obermeier for providing technical support. This project was partially funded by the DAAD, Germany (funding program 57507871), and the Department of Conservative Dentistry and Periodontology, Ludwig Maximilians University Munich, Germany.

References

1. Goodacre CJ, Eugene Roberts W, Munoz CA. Noncarious cervical lesions: morphology and progression, prevalence, etiology, pathophysiology, and clinical guidelines for restoration. *J Prosthodont* 2023;32:e1–18.
2. Yoshizaki KT, Francisconi-dos-Rios LF, Sobral MAP, Aranha ACC, Mendes FM, Scaramucci T. Clinical features and factors associated with non-carious cervical lesions and dentin hypersensitivity. *J Oral Rehabil* 2017;44:112–8.
3. Oginni AO, Adeleke AA. Comparison of pattern of failure of resin composite restorations in non-carious cervical lesions with and without occlusal wear facets. *J Dent* 2014;42:824–30.
4. Heintze SD, Ruffieux C, Rousson V. Clinical performance of cervical restorations—a meta-analysis. *Dent Mater* 2010;26:993–1000.
5. Duangthip D, Man A, Poon PH, Lo ECM, Chu CH. Occlusal stress is involved in the formation of non-carious cervical lesions. A systematic review of abfraction. *Am J Dent* 2017;30:212–20.
6. Kullmer O, Menz U, Fiorenza L. Occlusal fingerprint analysis (OFA) reveals dental occlusal behavior in primate molars. In: Thomas Martin, ed. *Mammalian teeth – form and function*, 1st ed. Munich: Verlag Dr. Friedrich Pfeil, 2020:25–43.
7. Correia A, Bresciani E, Borges A, Pereira D, Maia L, Caneppele T. Do tooth- and cavity-related aspects of non-carious cervical lesions affect the retention of resin composite restorations in adults? A systematic review and meta-analysis. *Operat Dent* 2020;45:E124–40.
8. Rees JS, Jacobsen PH. The effect of cuspal flexure on a buccal Class V restoration: a finite element study. *J Dent* 1998;26:361–7.

9. Benazzi S, Nguyen HN, Kullmer O, Kupczik K. Dynamic modeling of tooth deformation using occlusal kinematics and finite element analysis. *PLoS One* 2016;11:e0152663.
10. Soares P, Machado A, Zeola L, et al. Loading and composite restoration assessment of various non-cariou cervical lesions morphologies – 3D finite element analysis. *Aust Dent J* 2015; 60:309–16.
11. Rees JS, Jacobsen PH. The effect of interfacial failure around a class V composite restoration analysed by the finite element method. *J Oral Rehabil* 2000;27:111–6.
12. Masoudi Nejad R, Ghahremani Moghadam D, Ramazani Moghadam M, Aslani M, Asghari Moghaddam H, Mir M. Fracture behavior of restored teeth and cavity shape optimization: numerical and experimental investigation. *J Mech Behav Biomed Mater* 2021;124:104829.
13. Li H, Li J, Zou Z, Fok ASL. Fracture simulation of restored teeth using a continuum damage mechanics failure model. *Dent Mater* 2011;27:e125–33.
14. Tseng PC, Chuang SF, Kaisarly D, Kunzelmann KH. Simulating the shrinkage-induced interfacial damage around class I composite resin restorations with damage mechanics. *Dent Mater* 2023;39:513–21.
15. Hong HH, Liu HL, Hong A, Chao P. Inconsistency in the crown-to-root ratios of single-rooted premolars measured by 2D and 3D examinations. *Sci Rep* 2017;7:16484.
16. de France Électricité. *Finite element code_aster, analysis of structures and thermomechanics for studies and research*. 2021. Published online.
17. Lorentz E. A mixed interface finite element for cohesive zone models. *Comput Methods Appl Mech Eng* 2008;198:302–17.
18. Ferrari M, Goracci C, Sadek F, Cardoso PEC. Microtensile bond strength tests: scanning electron microscopy evaluation of sample integrity before testing. *Eur J Oral Sci* 2002;110: 385–91.
19. Kaisarly D, El Gezawi M, Lai G, Jin J, Rösch P, Kunzelmann KH. Effects of occlusal cavity configuration on 3D shrinkage vectors in a flowable composite. *Clin Oral Invest* 2018;22:2047–56.
20. Ausiello P, Ciaramella S, Di Rienzo A, Lanzotti A, Ventre M, Watts DC. Adhesive class I restorations in sound molar teeth incorporating combined resin-composite and glass ionomer materials: CAD-FE modeling and analysis. *Dent Mater* 2019;35: 1514–22.
21. Zeola L, Pereira F, Machado A, et al. Effects of non-cariou cervical lesion size, occlusal loading and restoration on biomechanical behaviour of premolar teeth. *Aust Dent J* 2016; 61:408–17.
22. Guo YB, Bai W, Liang YH. Fracture resistance of endodontically treated teeth with cervical defects using different restorative treatments. *J Dent Sci* 2022;17:842–7.
23. Song JH, Wang H, Belytschko T. A comparative study on finite element methods for dynamic fracture. *Comput Mech* 2008;42: 239–50.
24. Ichim I, Li Q, Loughran J, Swain M, Kieser J. Restoration of non-cariou cervical lesions part I. modelling of restorative fracture. *Dent Mater* 2007;23:1553–61.
25. Ichim I, Schmidlin P, Li Q, Kieser J, Swain M. Restoration of non-cariou cervical lesions part II. restorative material selection to minimise fracture. *Dent Mater* 2007;23:1562–9.
26. Hollanders ACC, Kuper NK, Huysmans MC, Versluis A. The effect of occlusal loading on cervical gap deformation: a 3D finite element analysis. *Dent Mater* 2020;36:681–6.
27. Schulz-Kornas E, Tittel M, Schneider H, et al. Tooth-composite bond failure with a universal and an etch-and-rinse adhesive depending on mode and frequency of application. *Dent Mater* 2024;40:359–69.
28. Haak R, Schmidt P, Park KJ, et al. OCT for early quality evaluation of tooth–composite bond in clinical trials. *J Dent* 2018; 76:46–51.
29. Haak R, Schäfer P, Hanßen B, et al. OCT Evaluation of marginal and internal interface integrity of class V composite restorations after 36 to 48 months. *J Adhesive Dent* 2022;24:165–74.
30. Merle CL, Fortenbacher M, Schneider H, et al. Clinical and OCT assessment of application modes of a universal adhesive in a 12-month RCT. *J Dent* 2022;119:104068.
31. Correia A, Andrade M, Tribst J, Borges A, Caneppele T. Influence of bulk-fill restoration on polymerization shrinkage stress and marginal gap formation in class V restorations. *Operat Dent* 2020;45:E207–16.
32. Sakaguchi RL, Ferracane JL, Powers JM, eds. *Craig's restorative dental materials*, 14th ed. St. Louis: Elsevier, 2019.
33. Ilie N, Hickel R. Investigations on mechanical behaviour of dental composites. *Clin Oral Invest* 2009;13:427–38.
34. Tam LE, Pilliar RM. Fracture toughness of dentin/resin-composite adhesive interfaces. *J Dent Res* 1993;72:953–9.
35. Hanabusa M, Mine A, Kuboki T, et al. Bonding effectiveness of a new 'multi-mode' adhesive to enamel and dentine. *J Dent* 2012;40:475–84.
36. Pongprueksa P, De Munck J, Karunratanakul K, et al. Dentin bonding testing using a mini-interfacial fracture toughness approach. *J Dent Res* 2016;95:327–33.
37. Rosa WLdO da, Piva E, Silva AF da. Bond strength of universal adhesives: a systematic review and meta-analysis. *J Dent* 2015; 43:765–76.
38. Serkies KB, Garcha R, Tam LE, De Souza GM, Finer Y. Matrix metalloproteinase inhibitor modulates esterase-catalyzed degradation of resin–dentin interfaces. *Dent Mater* 2016;32: 1513–23.

5. Publication 3

Direct ink writing with dental composites: A paradigm shift toward sustainable chair-side production

Po-Chun Tseng, Dar-Bin Shieh, Andreas Kessler,
Dalia Kaisarly, Peter Rösch, Karl-Heinz Kunzelmann,

Dent Mater 2024;40:1753–61.

<https://doi.org/10.1016/j.dental.2024.08.002>.



Direct ink writing with dental composites: A paradigm shift toward sustainable chair-side production

Po-Chun Tseng^{a,*}, Dar-Bin Shieh^{b,c,d}, Andreas Kessler^{a,f}, Dalia Kaisarly^a, Peter Rösch^e, Karl-Heinz Kunzelmann^a

^a Department of Conservative Dentistry and Periodontology, University Hospital, LMU Munich, Munich, Germany

^b School of Dentistry and Institute of Oral Medicine, National Cheng Kung University, Tainan, Taiwan

^c Center of Applied Nanomedicine and Core Facility Center, National Cheng Kung University, Tainan, Taiwan

^d Department of Stomatology, National Cheng Kung University Hospital, Tainan, Taiwan

^e Faculty of Computer Science, Technical University of Applied Sciences, Augsburg, Germany

^f Department of Prosthetic Dentistry, Faculty of Medicine, Center for Dental Medicine, Medical Center-University of Freiburg, Freiburg, Germany

ARTICLE INFO

Keywords:

Direct ink writing
3D printing
Additive manufacturing
Resin composites
Accuracy

ABSTRACT

Objectives: To evaluate the dimensional accuracy of occlusal veneers printed using a novel direct ink writing (DIW) system and a clinically approved dental composite.

Methods: A novel three-dimensional printer was developed based on the extrusion-based DIW principle. The printer, constructed primarily with open-source hardware, was calibrated to print with a flowable resin composite (Beautiful Flow Plus). The feasibility of this technology was assessed through an evaluation of the dimensional accuracy of 20 printed occlusal veneers using a laboratory confocal scanner. The precision was determined by pairwise superimposition of the 20 prints, resulting in a set of 190 deviation maps used to evaluate between-sample variations.

Results: Without material waste or residuals, the DIW system can print a solid occlusal veneer of a maxillary molar within a 20-minute timeframe. Across all the sampled surface points, the overall unsigned dimensional deviation was $30.1 \pm 20.2 \mu\text{m}$ (mean \pm standard deviation), with a median of $24.4 \mu\text{m}$ (interquartile range of $22.5 \mu\text{m}$) and a root mean square value of $36.3 \mu\text{m}$. The pairwise superimposition procedure revealed a mean between-sample dimensional deviation of $26.7 \pm 4.5 \mu\text{m}$ (mean \pm standard deviation; $n = 190$ pairs), indicating adequate precision. Visualization of the deviation together with the nonextrusion movements highlights the correlation between high-deviation regions and material stringing.

Significance: This study underscores the potential of using the proposed DIW system to create indirect restorations utilizing clinically approved flowable resin composites. Future optimization holds promise for enhancing the printing accuracy and increasing the printing speed.

1. Introduction

Composite resin restorations have become a viable treatment modality in various clinical scenarios. Direct resin composites have proven to be consistently successful in the complete rehabilitation of severely worn teeth [1,2]. However, extensive defects remain challenging, mainly due to the complexity of achieving ideal occlusions and contours [3]. Moreover, the stress generated during the polymerization of bulk resin composites poses a threat to the bonding interface, potentially compromising clinical longevity [4,5]. Indirect restorations are options for the treatment of extensive defects to reduce the level of skill and time

required to perform layering while still achieving optimal results.

Despite the clear advantages of indirect restorations, there are still significant disadvantages to traditional laboratory fabrication, such as high costs and additional visits. In response to these challenges, computer-aided manufacturing (CAM) systems have been introduced to dentistry. Shaping can be achieved through subtractive or additive approaches. Although subtractive systems have long demonstrated clinical success, they are linked to significant material waste, tool attrition, initial investments, and high production costs [6,7]. Consequently, researchers are turning their attention to additive manufacturing (AM) for enhanced sustainability and affordability in dental applications [7,8].

* Correspondence to: Department of Conservative Dentistry and Periodontology, University Hospital, LMU Munich, Goethestr. 70, 80336 Munich, Germany.
E-mail address: P.Tseng@campus.lmu.de (P.-C. Tseng).

<https://doi.org/10.1016/j.dental.2024.08.002>

Received 3 February 2024; Accepted 1 August 2024

Available online 7 August 2024

0109-5641/© 2024 The Authors. Published by Elsevier Inc. on behalf of The Academy of Dental Materials. This is an open access article under the CC BY license (<http://creativecommons.org/licenses/by/4.0/>).

Additive manufacturing, or three-dimensional (3D) printing, has excellent potential to reduce material waste and lower production costs. Most research and innovations in restorative dentistry currently rely on vat photopolymerization techniques [9]. In these techniques, 3D objects are created by selectively casting polymerizing light onto resin reservoirs. While this approach is utilized in the fabrication of resin-based restorations, it is compatible only with resins with low filler contents due to viscosity constraints [10]. This limitation, in turn, restricts the mechanical properties of printed objects. In addition, after printing, the meticulous postprocessing of printed objects is needed, which includes removal of the residual resin from the object surface using organic solvents and postcuring to improve the mechanical properties of the objects [9]. This cleaning process may inadvertently release hazardous chemicals into the environment and expose dental professionals to ultrafine particles [11,12]. This raises concerns about the potential allergenicity and toxicity of these substances [13].

In this paper, an innovative direct-ink writing (DIW) technology is proposed to overcome the limitations associated with existing techniques. DIW precisely deposits controlled amounts of high-viscosity materials through an extrusion process [14], so highly filled materials can be used for the production of mechanically robust definitive restorations. In particular, this approach reduces occupational exposure to resin chemicals and minimizes the environmental impact by producing virtually no byproducts [15,16]. The recent expiration of patents for DIW technology has made DIW a cost-effective way of producing durable and sustainable indirect restorations [17].

Despite the advantages of the DIW technique, its application in restorative dentistry remains largely unexplored. To support the on-demand production of indirect restorations, we developed a DIW AM system capable of printing with a flowable dental composite. Continuous blue-light illumination was incorporated to solidify the extruded resin composite, preventing material slumping and enabling high-fidelity printing for definitive restorations [18,19]. The DIW approach eliminates the need for postprocessing and machine cleaning, resulting in an efficient and environmentally friendly fabrication process [15]. In addition, we utilized clinically approved material for posterior restorations to minimize the gap to chairside applications. As a pioneering use of DIW for dental composites, the proposed method provides a new avenue for the sustainable and point-of-care production of definitive restorations.

The primary objective of this study was to design and optimize a novel DIW system tailored to printing with a flowable composite. Rigorous assessments of dimensional accuracy were conducted to ensure the system's reliability and clinical feasibility. Moreover, our printer design is accessible to the research community via the Open Science Framework repository, further fostering cross-border collaborations toward affordable indirect restorations [20].

2. Materials and methods

2.1. Machine settings

An experimental 3D printing system was developed based on the DIW principle. The printer builds 3D structures layer by layer using an extruder (Preeflow® eco-PEN 300, ViscoTec, Töging am Inn, Germany) and a nozzle with an interior diameter of 340 μm (Micron-S dispensing tip, Vieweg, Kranzberg, Germany). During printing, the extruder moves only vertically, and the sample platform moves horizontally based on CoreXY kinematics [21]. To gain direct control over the printing process, the extruder's proprietary motor was replaced by a standard stepper motor. The printer was operated with an Arduino Mega 2560 microcontroller and a RAMPS 1.4 extension board, allowing precise optimization of the printing parameters. Furthermore, two blue-light light-emitting diode (LED) modules (DO-BDL 8W-2A, Osram, Regensburg, Germany) were integrated to provide concurrent light-initiated polymerization. This feature ensured rapid solidification of the

composite material and reduced slumping during the printing process. The design of the printer is available at <https://doi.org/10.17605/OSF.IO/K2Z5S>.

2.2. Tuning process

The DIW printing system was calibrated for the precise extrusion of a flowable dental composite (Beautifil Flow Plus F00A3, lot 052178, Shofu, Inc., Kyoto, Japan). Consisting of Bis-GMA, TEGDM, and a filler load of 47 % by volume [22], the composite can also be used for posterior restorations. The tuning process focused on determining the optimal step rate and extrusion volume. Furthermore, continuous blue-light irradiation was applied while ensuring no clogging of the nozzle. All the printed samples were thinly powdered and characterized using a chromatic confocal scanner (KF-30, Syndicat Ingenieurbüro, Munich, Germany) with a scanning resolution of 20 μm in the horizontal direction and an accuracy of 1.5 μm in the vertical direction.

The cross-sectional area of the printed lines was measured to assess the flow of the composite material through the nozzle to ensure consistent and uniform flow. Further adjustments to the printing parameters were made based on the dimensions and flatness of the printed cylinders. Through iterative refinement, scaling factors of 1.5 % in the y-direction and 1 % in the x-direction were established to compensate for polymerization shrinkage.

2.3. Printing and deviation characterization

The occlusal surface of a maxillary first molar model was sliced to generate G-code using Ultimaker Cura (version 5.0.0) with a layer thickness of 100 μm and 100 % infill. The object was constructed layer-by-layer in a sequence of increasing heights, with the infill printed before the respective outer walls within each enclosed region. Since the structure was solid with a flat bottom, no supplementary support structures were required for this investigation. The printed occlusal veneers were postcured for 20 s immediately after printing using a dental light-curing unit (Bluephase style, Ivoclar Vivadent, Schaan, Liechtenstein) with an output exceeding 1000 mW/cm^2 . After 24 h, the restorations ($n = 20$) were finely powdered and digitized using the KF-30 scanner.

The 3D scans were imported into ImageJ software as height maps, where the gray value of each pixel represented the vertical height. To mitigate speckle noise resulting from specular reflection, pixels exhibiting white noise were selectively processed using a median filter. The raster images were then saved in TIFF format for subsequent 3D analysis.

For deviation calculations, the images were imported into the open-source software CloudCompare (version 2.12.4) as individual 3D point clouds. The clouds were first roughly aligned with the reference mesh and then registered to the reference using the iterative closest point algorithm without a scaling operation [23]. The deviation of the registered clouds from the reference was computed using the cloud-to-cloud distance algorithm [24]. Data from the lowest layer (less than 100 μm in height) were cropped and removed to reduce measurement inaccuracies in steeply inclined regions [25].

Accuracy consists of trueness and precision. Trueness reflects the extent to which the measured objects deviate from designated dimensions, as defined in the reference model. To assess trueness, the cloud-to-cloud distances between the virtual reference model and each sample were used to create trueness maps (Fig. 1a). Additionally, precision reflects the closeness between two independent samples (Fig. 1d) [26]. Consequently, 190 nonrepetitive pairs were derived from the 2-combinations of the 20 samples. For each pair, the point clouds were aligned to one another, a process also referred to as pairwise superimposition. The cloud-to-cloud distances between the two aligned clouds were subsequently computed to produce precision maps.

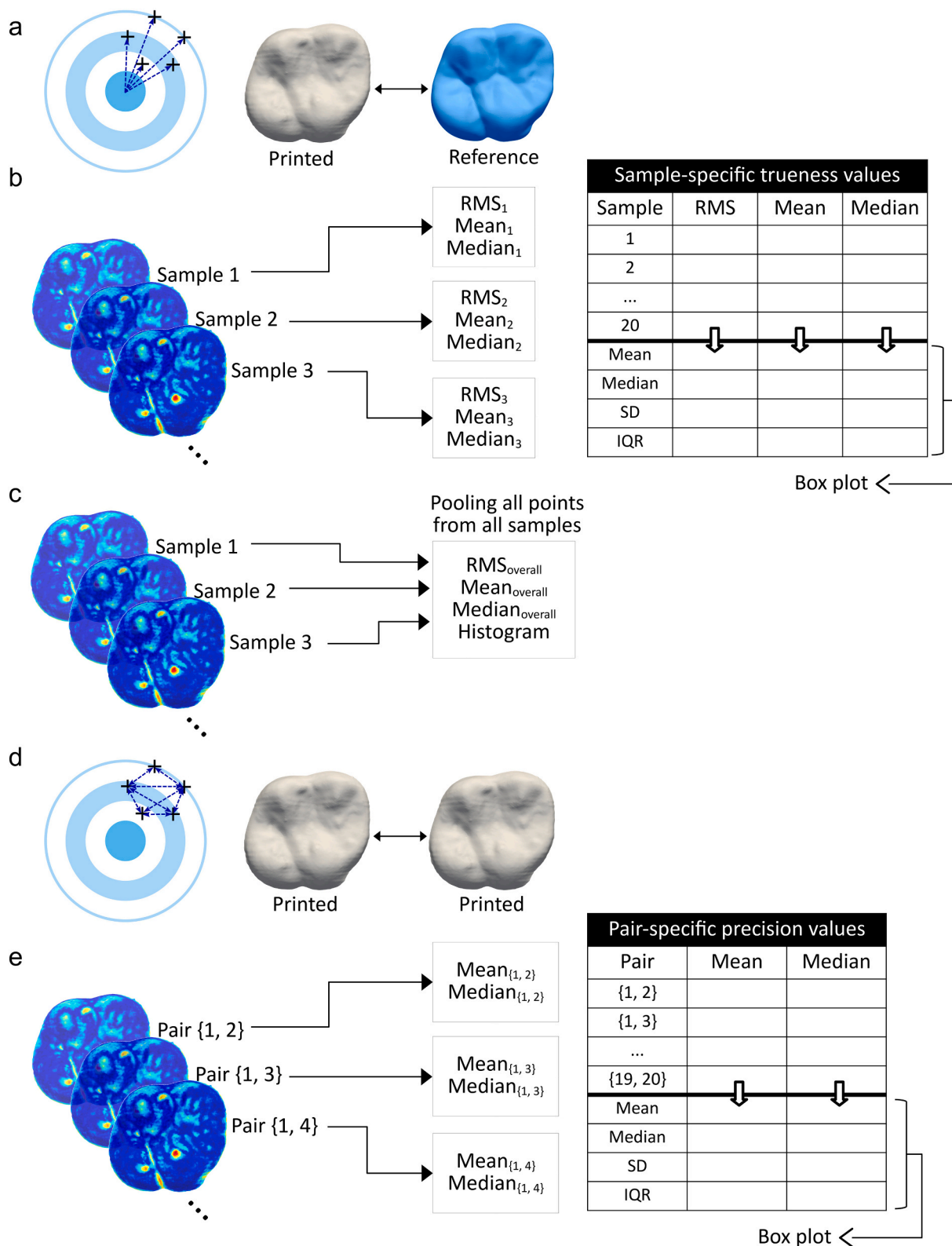


Fig. 1. Schematics illustrating the computation of accuracy in this study. Three sets of statistics are provided to define sample-specific trueness, overall trueness, and pair-specific precision. (a) The trueness is derived from the dimensional deviation of the samples from the reference model. (b) In the conventional approach, deviation data for each sample are preprocessed via arithmetic aggregation operations, generating sample-specific trueness for subsequent statistical analysis. However, in the aggregation process, all within-sample spatial variability is eliminated. (c) To incorporate within-sample deviation variability into the analysis, the surface-wide deviation data for all samples are pooled together to obtain an overall histogram and statistics. This approach provides an efficient and comprehensive overview of the range of deviation across all surfaces. (d) Precision illustrates the differences between each pair of samples. Notably, the 20 samples are superimposed in a pairwise manner, leading to 190 deviation maps. (e) The pair-specific precision is derived through aggregation operations on the deviation maps, similar to preprocessing for sample-specific trueness. RMS: root mean square, SD: standard deviation, IQR: interquartile range.

2.4. Accuracy statistics and visualization

The collected data were statistically analyzed using the software R (version 4.0.2). For trueness evaluation, the sample-specific means and medians of the deviations were derived by preprocessing surface-wide deviation data on a per-sample basis for subsequent statistical analysis (Fig. 1b). The root mean square (RMS) values of the data were presented as a measure of accuracy [27]. Considering that the preprocessing procedure eliminated within-sample spatial variability, additional statistics were provided based on pooled surface-wide deviation data from all samples (Fig. 1c), thereby incorporating spatial components of variability into the analysis.

To assess precision across multiple samples, pair-specific arithmetic means and medians were computed for each deviation map generated by pairwise superimposition (n = 190 pairs; Fig. 1e). The sample-specific trueness and pair-specific precision were then summarized in a box plot, providing an overview of the dimensional accuracy metrics at the sample level. Furthermore, the pooled data are presented in a histogram to illustrate their overall statistical distribution.

Statistics alone provide no information on the spatial distribution of the deviation. For visualization, a surface was reconstructed based on a representative sample using the Poisson surface reconstruction algorithm. The previously derived dimensional deviation for a given cloud was mapped to the reconstructed surface to obtain a 3D deviation heat map. As high deviation points were concentrated in certain areas, the G-codes were analyzed to determine what was occurring in those regions. In particular, nonextrusion movements of the extruder were extracted from the G-codes and superimposed on the deviation heat map to help explain the deviation pattern.

3. Results

3.1. Machine cost and production speed

The hardware cost for the DIW printing system was less than 5000 euros. No costs were incurred for the software, as open-source software was used. Personnel costs were not accounted for (Fig. 2a). The system demonstrated that it is capable of printing an occlusal veneer in a time frame of 20 min (Fig. 2b). Notably, the printing process produced minimal material waste because only the required quantities of resin composites were extruded and residue was mitigated. The efficient use of materials contributes to the sustainability and cost efficiency of the printing process.

3.2. Accuracy evaluation

The dimensional accuracy of the printed occlusal veneers was quantitatively evaluated, and the results are summarized in Table 1. As illustrated in Fig. 1, three sets of statistics were provided to assess trueness and precision.

A common approach to analyzing data from multiple samples is to arithmetically preprocess the surface-wide deviation data at the sample level, yielding aggregated sample-specific accuracy metrics for subsequent statistics. A box plot (Fig. 3a) was created to present the sample-specific RMS, mean, and median of the dimensional deviations, with these aggregated metrics illustrated across all samples (n = 20). The results indicate a high level of consistency among samples, as evidenced by the minimal variability in terms of sample-specific trueness.

In the second analysis, surface-wide deviation data from all samples were pooled together to include within-sample spatial variability for the overall statistics. The mean dimensional deviation was $30.1 \pm 20.2 \mu\text{m}$ (mean \pm SD), with an RMS of $36.3 \mu\text{m}$. The median deviation was $24.4 \mu\text{m}$, and the IQR was $22.5 \mu\text{m}$. As shown in the histogram (Fig. 3b), the distribution is slightly positively skewed, demonstrating an elongated tail on the right side of the distribution.

For precision, the dimensional deviation between every combination of the two prints was computed through pairwise superimposition and pair-specific aggregation. The mean deviation was $26.7 \pm 4.5 \mu\text{m}$ (mean \pm SD), while the median was $22.6 \pm 2.9 \mu\text{m}$ (mean \pm SD). More detailed statistics are shown in Table 1. The precision values suggest

Table 1
Accuracy statistics.

Sample-Specific Trueness			
Metrics	Mean (SD)	Median (IQR)	95th Percentile
RMS	36.2 (2.6)	35.9 (4.0)	39.3
Mean	30.1 (1.9)	29.9 (3.1)	32.3
Median	24.5 (1.3)	24.2 (1.7)	26.1
Pooled Overall Trueness			
Metrics	Mean (SD)	Median (IQR)	95th Percentile
RMS	36.3	24.4 (22.5)	70.5
Mean	30.1 (20.2)		
Precision by Pairwise Superimposition			
Metrics	Mean (SD)	Median (IQR)	95th Percentile
Mean	26.7 (4.5)	25.3 (8.7)	34.2
Median	22.6 (2.9)	21.7 (5.0)	27.5

Units are in μm . RMS: root mean square, SD: standard deviation, IQR: inter-quartile range.

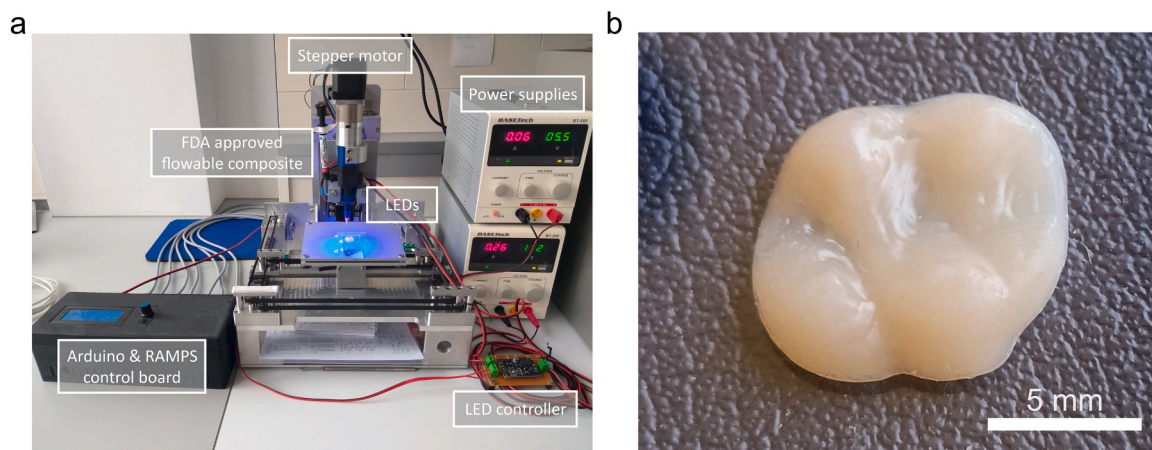


Fig. 2. Machine settings for the 3D printer and a printed occlusal veneer. (a) The printer is built primarily using open-source hardware components. The extruder moves only in the vertical direction to reduce vibration caused by the movement of relatively heavy parts. Blue-light LEDs are installed to provide instantaneous polymerization. (b) The occlusal veneer can be printed within 20 min using a clinically approved flowable composite.

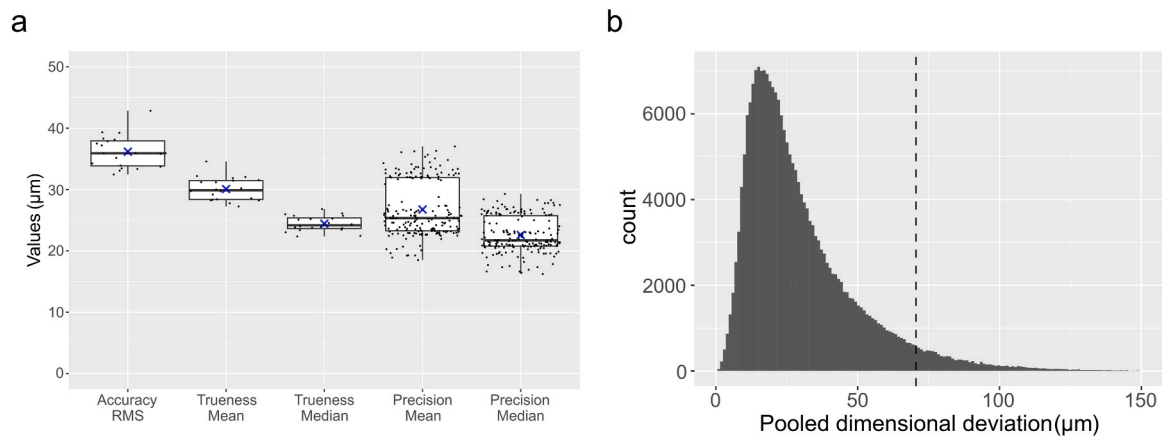


Fig. 3. Box plot of the accuracy metrics and histogram of the overall deviation. (a) Box plots of sample-specific trueness ($n = 20$) and pair-specific precision ($n = 190$ pairs). The deviation data are first preprocessed at the sample or pair level using the root mean square (RMS), mean, or median values. The mean values of the boxes are denoted by blue crosses. (b) Histogram illustrating the overall dimensional deviation of all the sampled surfaces. To retain the within-sample spatial variability of deviation, the raw data are pooled without aggregation preprocessing. The dashed line indicates the location of the 95th percentile.

sufficient reproducibility among prints. These precision metrics, also depicted in the box plot (Fig. 3a), provide information on the extent of between-sample variability among the restorations.

3.3. Visualization of deviations

In addition to the statistical distribution and metrics of the dimensional deviation, the spatial distribution of the deviation was visualized for a representative sample. The reference model (Fig. 4a) is presented along with the representative sample (Fig. 4b). As shown in the deviation map (Fig. 4c), the regions of high deviation are concentrated at the palatal groove and several excessive protuberances on the cusps, thus contributing to the positive skewness in the histograms (Fig. 3b and Fig. 4d).

To determine the cause of the protuberances, the nonextrusion movements of the extruder were extracted from the G-codes and superimposed on the deviation map. As shown in Fig. 4e, regions with high deviations were located primarily above the sites where the extruder moved across the outer walls of one printed region to approach the next printing region. Thus, the inaccurate protuberances were likely caused by material "stringing" at the "perimeter-crossing" sites (Fig. 4f).¹

4. Discussion

In this study, the potential of using DIW technology for the on-demand fabrication of indirect resin composite restorations is demonstrated. While ceramics are generally more wear resistant than resin composites, the latter remain attractive alternatives because of their ease of repair and replacement [28]. The experimental printer demonstrated the capability to produce a posterior veneer within 20 min, with high dimensional accuracy. By further optimizing and mass-producing the system, higher printing speeds and lower machine costs could be achieved. To our knowledge, this study represents the first application of DIW technology in producing composite resin restorations. By utilizing clinically approved materials and open hardware, our approach aims to make indirect restorations affordable and accessible to a wide range of patients.

¹ "Perimeter" is defined as the outline of an outer surface or wall of a printed object. A printed object can have several perimeters. In the context of an occlusal surface, each cusp possesses a distinct perimeter. The term "stringing" refers to material being pulled from the printed area, forming a thin string. When the extruder moves from one cusp to the next, "perimeter crossing" may cause "stringing".

Despite the global trend of decreased incidence of caries, an increasing demand for indirect restorations is expected in an aging society. A systematic review suggested that approximately 17 % of adults may have severe tooth wear by the age of 70 [29]. If left untreated, damage can lead to problems such as dentin exposure, hypersensitivity, and even alterations to occlusion. Ensuring affordable access to high-quality indirect restorations will be critical to overcome this emerging challenge.

In addition to addressing unmet needs, the DIW system was developed with a particular focus on sustainability, considering environmental, economic, and social factors. To ensure sustainable prosperity for both humanity and the planet, the United Nations has outlined seventeen Sustainable Development Goals (SDGs) in their 2030 Agenda [30]. Nevertheless, these sustainability concepts have yet to be fully integrated into dental practice [31].

This study represents a pivotal step toward more sustainable restorative dentistry. From an environmental perspective, the DIW approach reduces residual resin waste and improves the management of hazardous chemicals. The point-of-care DIW system will contribute to reducing the carbon footprint associated with transportation between dental clinics and laboratories [32]. In addition, the overall cost of the system can be significantly reduced through mass-production and further adoption of open-hardware components [16], thus advancing health equity for social sustainability. The open-science approach further contributes to economic sustainability by fostering global partnerships and domestic innovations [33,34]. Consequently, the study reflects a practical paradigm shift toward equitable long-term prosperity for future generations.

In recent years, the landscape of restorative dentistry has evolved significantly with the application of additive manufacturing. One noteworthy development was the introduction of a filled resin by Bego, which was designed for vat photopolymerization to create definitive composite resin restorations. This product holds promise for printing with filled composites using established methods, with favorable outcomes in terms of marginal adaptation and biocompatibility [7,35]. However, importantly, the filler size of this product is similar to that of microfilled composites, and the filler content remains lower than that of most flowable composites [36]. Since microfilled composites with low filler contents may exhibit low wear resistance and poor mechanical properties, further studies are warranted to evaluate the in vitro and clinical performance of these novel materials [37,38].

In pursuit of restorations with improved wear resistance and mechanical properties, researchers have focused on the AM of zirconia ceramics and polymer-infiltrated ceramic network (PICN) composites

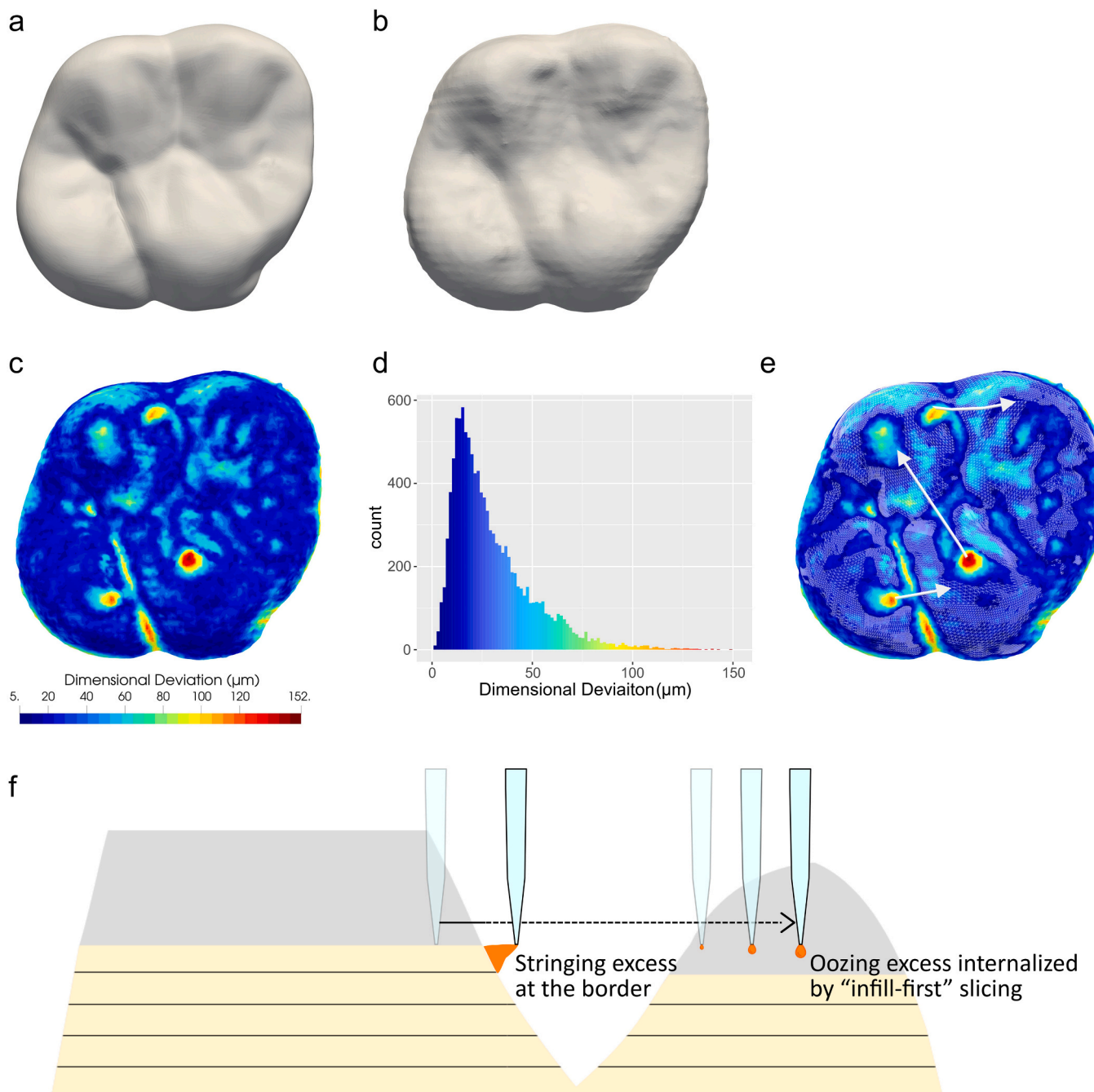


Fig. 4. Reference model and the dimensional deviation of a representative printed object. (a) Reference model. (b) Surface reconstructed from the point cloud of a representative sample. (c) Color map of the representative sample, illustrating its dimensional deviation from the reference model. (d) Deviation histogram of the representative sample. (e) Deviation map with the superimposed reference model shown as a white mesh. Areas without mesh indicate an excess amount of material. Additionally, nonextruding printing paths (white solid lines) imported from the G-codes are used to elucidate the link between material stringing and high-deviation areas. (f) Schematic diagram illustrating the concepts of stringing and oozing. When the extruder leaves the printed region, the nozzle drags a trace amount of viscoplastic composite from the border, leading to an excess; this process is referred to as the stringing phenomenon (left). On the other hand, the residual hydrostatic pressure within the nozzle causes material to ooze during long nonextrusion movements (right). The dimensional deviation from the oozing effect is minimized by adopting an “infill-first” slicing strategy, which initiates the printing of new regions from the infill and internalizes the excess oozed material. The same color scale applies to (c), (d), and (e).

[39]. A recent publication reported a promising sub-100 μm surface deviation in stereolithographic-printed zirconia restorations [40]. However, importantly, the drying process required for these materials is energy-intensive and time-consuming, posing challenges for on-demand applications. In addition, vat photopolymerization techniques often result in substantial residual resin remnants, highlighting the necessity of an alternative approach to facilitate the clean and on-demand

production of definitive restorations.

To overcome these limitations, we opted for a different approach using DIW with resin composites. Despite the use of serial rather than parallel production, our approach is a viable option for chairside applications because it eliminates the need for time-consuming post-processing [40]. While prior studies employed the DIW technique to print resin-based tooth-like structures, the clinical relevance of this

technique was limited; notably, the structures were printed with experimental hydroxyapatite resin composites, and the reported dimensional accuracy has yet to reach a clinically acceptable level [41, 42]. Thus, our primary objective was to investigate the feasibility of using DIW technology to produce resin composites in a clinically relevant context.

In our study, multiple accuracy metrics are used to fully assess the capability of the novel printing system (Table 1). The largest values were reported by the RMS, as it gives greater weight to larger values in the input data than do other metrics. Although commonly used to assess accuracy, the RMS calculation incorporates both variance and arithmetic mean components [43]. On the other hand, medians yield the smallest value in a right-skewed distribution, as extreme values have limited effects. Considering the nonnormal nature of an unsigned deviation, the median emerges as a suitable descriptor for trueness in this study. The observed differences among the trueness metrics indicate the need for more standardized statistics to enhance comparability among 3D printing studies [26].

Studies of digital manufacturing techniques often focus on trueness evaluation without reporting precision metrics [6,10,27,40,44]. By definition, precision reflects the agreement between independent test results or samples. As the variability statistics of the pooled deviation data reflect the variability in trueness across all sample points, they do not strictly represent precision [26]. To exclude within-sample trueness variability from calculations, pairwise superimposition is commonly employed to illustrate differences in individual pairs of scans [26]. However, pairwise operations generate numerous superimposition maps, posing challenges to implementation and subsequent outcome visualization. There is a need for an intuitive way to compute multi-sample precision and visualize the corresponding results in 3D to enhance the reliability of digital technologies in restorative dentistry.

In addition to the differences in trueness metrics, the effects of data aggregation on variability statistics are considered in this study. As shown in Table 1, the variability values of the overall trueness metrics consistently surpass those of the corresponding sample-specific metrics. From a statistical perspective, sample-specific metrics are based on aggregated data, where each sample is represented by its RMS, mean, and median deviation. While aggregation preprocessing serves to provide a concise overview of complex multilevel data, low-level variations are discarded, resulting in considerably smaller dispersion values.

Drawing an analogy to economics, the gross domestic product (GDP) per capita represents an aggregated value of produced goods and services divided by a country's average population. This definition is used to effectively highlight differences at the country level but overlooks variations among individual residents. Similarly, in studies of dimensional deviation, presenting statistics based on sample-specific trueness metrics offers insights into aggregated values at the sample level but fails to capture variability in within-sample deviations.

To illustrate the within-sample variability, an "overall" histogram and corresponding statistics derived from pooled surface-wide deviation data for all samples are obtained (Fig. 3b). This approach retains within-sample spatial variability, facilitating efficient parameter fine-tuning for accurate shapes. Specifically, the positively skewed distribution of the overall histogram suggests that only a small portion of the surface is characterized by a high deviation. A meticulous examination of the deviation maps was further performed to identify the high-deviation regions, which were protuberances caused by material excess. Statistical analysis was integrated with spatial visualization to optimize the printing accuracy. By overlaying the nonextrusion movements of the extruder onto the representative deviation map (Fig. 4e), we established the connection between the region of excess material and material stringing. This workflow not only enhances our understanding of dimensional deviations but also offers valuable insights for improving the printing accuracy.

Stringing, a broadly recognized phenomenon in extrusion-based 3D printing, is often confused with the term "oozing" in the 3D printing

community. While both terms are associated with undesired material excess, it is crucial to delineate their distinctions to achieve high-accuracy printing. Oozing is an overextrusion resulting from the release of accumulated internal hydrostatic pressure [45]. This phenomenon tends to be prominent after nonextrusive movements. On the other hand, stringing is caused by the outward pulling of viscous materials and predominantly occurs as the extruder departs from the border of the printed region (also referred to as the perimeter) and moves toward the next printing region.

In this study, we alleviated the oozing problem by implementing an "infill-first" slicing strategy. In infill-first slicing, the extruder is directed to the inner part of the next printing region immediately after completing printing in the previous region; thus, the oozed excess is internally contained, and the deviation resulting from oozing is minimized. In contrast, managing the stringing phenomenon is more challenging because it is primarily affected by the viscosity of the material. Nevertheless, small regions of excess can be readily identified and corrected by clinicians. Moreover, optimizing the printing paths to reduce the number of perimeter-crossing events is a potential solution for the stringing problem [46].

The current study demonstrated the potential of DIW technology for use in the production of permanent composite resin restorations. Our findings suggest that the DIW system is well suited for clinical applications in restorative dentistry. However, importantly, while the flowable composite used in this study can be used for class II cavities, composites with higher filler loads are generally preferred due to their superior mechanical properties [47]. To fully leverage the potential of DIW technology, ongoing research should focus on assessing the compatibility of the system with hybrid and universal composites.

Despite the promising results of this study, there are still aspects that require further investigation. First, to assess the performance of DIW printers, a comparative analysis with other manufacturing systems should be performed. This approach would provide a better understanding of the advantages and limitations of DIW in relation to existing technologies. Second, the integration of an additional extruder is recommended, as many restorations include unsupported parts that necessitate support from sacrificial structures. Finally, future research should aim to expand the scope of application by exploring the printing of various types of fixed prostheses and assessing their fitness. Addressing these questions will further enhance the potential of using DIW technology in restorative dentistry.

The accuracy of manufacturing depends on various factors, such as the technology, printer specifications, materials used, geometries, and specific region of interest. In addition, studies have noted the effects of printing parameters on dimensional accuracy [48]. Meaningful comparisons of the accuracy values across different publications can be achieved only after taking these factors into account. To facilitate effective communication and comparison, establishing a consensus regarding standardized print geometry and statistics would be highly advantageous [26]. These benchmarks provide a foundation for future studies, enabling a more systematic approach to evaluating the accuracy of 3D printing technologies.

In conclusion, our study demonstrated the potential of using DIW technology in the on-demand production of indirect composite restorations. The analysis indicated that the proposed DIW system can achieve a dimensional accuracy comparable to that of the current subtractive manufacturing systems [6,40]. Based on its multifaceted support of sustainability and the dimensional accuracy demonstrated, the proposed DIW approach should be further researched and improved.

Declaration of Generative AI and AI-assisted technologies in the writing process

Statement: During the preparation of this work the authors used ChatGPT, an artificial intelligence (AI) language model developed by OpenAI, in order to improve the language of this manuscript. After using

this service, the authors reviewed and edited the content as needed and take full responsibility for the content of the publication.

Acknowledgments

The authors would like to thank Mr. S. Ratzesberger for his initial work on the project, Mr. T. Obermeier for providing technical support and inspiration, and Mrs. G. Dachs and Mrs. E. Koebele for their efforts.

We would like to express sincere gratitude to Mr. Dipl.-Ing. Georg Hiebl, Syndicad Ingenieurbüro, Munich, Germany, for his support of this project, as he was constantly available to address any issues. Over the past 25 years of collaborative development of specialized dental testing machines, we have gained extensive knowledge in construction, mechanics, electronics, and programming. This collective experience enabled us to achieve the successful implementation of this project.

This project was partially funded by the DAAD, Germany (funding program S7507871 awarded to Po-Chun Tseng), and the Department of Conservative Dentistry and Periodontology, Ludwig-Maximilians-University of Munich, Germany. This study was also supported by a grant from the German Society of Restorative and Regenerative Dentistry (DGR²Z) and Kulzer. Furthermore, we acknowledge the support provided by the IADR Kulzer Travel Award and the travel grant from the Taiwan Association for Dental Sciences, which facilitated our participation in the 2023 IADR/LAR General Session.

References

- Mehta SB, Lima VP, Bronkhorst EM, Crins L, Bronkhorst H, Opdam NJM, et al. Clinical performance of direct composite resin restorations in a full mouth rehabilitation for patients with severe tooth wear: 5.5-year results. *J Dent* 2021; 112:103743. <https://doi.org/10.1016/j.jdent.2021.103743>.
- Loomans BAC, Kreulen CM, Huijs-Visser H, Sterenborg B, Bronkhorst EM, Huysmans M, et al. Clinical performance of full rehabilitations with direct composite in severe tooth wear patients: 3.5 Years results. *J Dent* 2018;70:97–103. <https://doi.org/10.1016/j.jdent.2018.01.001>.
- Angeletaki F, Gkogkos A, Papazoglou E, Kloukos D. Direct versus indirect inlay/onlay composite restorations in posterior teeth. A systematic review and meta-analysis. *J Dent* 2016;53:12–21. <https://doi.org/10.1016/j.jdent.2016.07.011>.
- Tseng P-C, Chuang S-F, Kaisarly D, Kunzelmann K-H. Simulating the shrinkage-induced interfacial damage around Class I composite resin restorations with damage mechanics. *Dent Mater* 2023;39:513–21. <https://doi.org/10.1016/j.dental.2023.03.020>.
- Hayashi J, Shimada Y, Tagami J, Sumi Y, Sadr A. Real-Time Imaging of Gap Progress during and after Composite Polymerization. *J Dent Res* 2017;96:992–8. <https://doi.org/10.1177/0022034517709005>.
- Al Hamad KQ, Al Rashdan RB, Al Rashdan BA, Al Quran FA. Effect of CAD-CAM tool deterioration on the trueness of ceramic restorations. *J Prosthet Dent* 2022; 127:635–44. <https://doi.org/10.1016/j.prosdent.2020.09.035>.
- Daher R, Ardu S, di Bella E, Krejci I, Duc O. Efficiency of 3D-printed composite resin restorations compared with subtractive materials: evaluation of fatigue behavior, cost, and time of production. *S0022391322004814 J Prosthet Dent* 2022. <https://doi.org/10.1016/j.prosdent.2022.08.001>.
- Hegeudus T, Kreuter P, Kismarci-Antalfy AA, Demeter T, Banyai D, Vegh A, et al. User experience and sustainability of 3d printing in dentistry. *Int J Environ Res Public Health* 2022;19:1921. <https://doi.org/10.3390/ijerph19041921>.
- Andjela L, Abdurahmanovich VM, Vladimirovna SN, Mikhailovna GI, Yurievich DD, Alekseevna MY. A review on Vat Photopolymerization 3D-printing processes for dental application. *Dent Mater* 2022;38:e284–96. <https://doi.org/10.1016/j.dental.2022.09.005>.
- Lin C-H, Lin Y-M, Lai Y-L, Lee S-Y. Mechanical properties, accuracy, and cytotoxicity of UV-polymerized 3D printing resins composed of Bis-EMA, UDMA, and TEGDMA. *J Prosthet Dent* 2020;123:349–54. <https://doi.org/10.1016/j.prosdent.2019.05.002>.
- Rodríguez-Hernández AG, Chiodoni A, Bocchini S, Vazquez-Duhalt R. 3D printer waste, a new source of nanoplastic pollutants. *Environ Pollut* 2020;267:115609. <https://doi.org/10.1016/j.envpol.2020.115609>.
- Felici G, Lachowicz JI, Milia S, Cannizzaro E, Cirrincione L, Congiu T, et al. A pilot study of occupational exposure to ultrafine particles during 3D printing in research laboratories. *Front Public Health* 2023;11:1144475. <https://doi.org/10.3389/fpubh.2023.1144475>.
- Walpitagama M, Carve M, Douek AM, Trestrail C, Bai Y, Kaslin J, et al. Additives migrating from 3D-printed plastic induce developmental toxicity and neuro-behavioural alterations in early life zebrafish (Danio rerio). *Aquat Toxicol* 2019; 213:105227. <https://doi.org/10.1016/j.aquatox.2019.105227>.
- Saadi MASR, Maguire A, Pottackal NT, Thakur MSH, Ikram MMD, Hart AJ, et al. Direct ink writing: a 3d printing technology for diverse materials. *Adv Mater* 2022; 34:2108855. <https://doi.org/10.1002/adma.202108855>.
- Rocha VG, Saiz E, Tirichenko IS, García-Tuñón E. Direct ink writing advances in multi-material structures for a sustainable future. *J Mater Chem A* 2020;8: 15646–57. <https://doi.org/10.1039/D0TA04181E>.
- Teegen I-S, Schadte P, Wille S, Adelung R, Siebert L, Kern M. Comparison of properties and cost efficiency of zirconia processed by DIW printing, casting and CAD/CAM-milling. *Dent Mater* 2023;39:669–76. <https://doi.org/10.1016/j.dental.2023.05.001>.
- Cesarano III J., Calvert P. Freeforming objects with low-binder slurry. 20015682, 2000.
- Vatani M, Choi J-W. Direct-print photopolymerization for 3D printing. *Rapid Prototyp J* 2017;23:337–43. <https://doi.org/10.1108/RPJ-11-2015-0172>.
- Farahani RD, Lebel LL, Therriault D. Processing parameters investigation for the fabrication of self-supported and freeform polymeric microstructures using ultraviolet-assisted three-dimensional printing. *J Micromech Microeng* 2014;24: 055020. <https://doi.org/10.1088/0960-1317/24/5/055020>.
- Foster ED, Deardorff A. Open Science Framework (OSF). *J Med Libr Assoc JMLA* 2017;105:203–6. <https://doi.org/10.5195/jmla.2017.88>.
- Peek N, Moyer I. Popfab: A case for portable digital fabrication. *Proc. Elev. Int. Conf. Tangible Embed. Embodied Interact.* Yokohama Japan: ACM; 2017. p. 325–9. <https://doi.org/10.1145/3024969.3025009>.
- Al Sunbul H, Silikas N, Watts DC. Polymerization shrinkage kinetics and shrinkage-stress in dental resin-composites. *Dent Mater* 2016;32:998–1006. <https://doi.org/10.1016/j.dental.2016.05.006>.
- Besl PJ, McKay ND. A method for registration of 3-D shapes. *IEEE Trans Pattern Anal Mach Intell* 1992;14:239–56. <https://doi.org/10.1109/34.121791>.
- Marcel R, Reinhard H, Andreas K. Accuracy of CAD/CAM-fabricated bite splints: milling vs 3D printing. *Clin Oral Invest* 2020;24:4607–15. <https://doi.org/10.1007/s00784-020-03329-x>.
- Mehl A, Gloger W, Kunzelmann K-H, Hickel R. A new optical 3-d device for the detection of wear. *J Dent Res* 1997;76:1799–807. <https://doi.org/10.1177/0022034597076011201>.
- Mehl A, Reich S, Beuer F, Güth J-F. Accuracy, trueness, and precision - a guideline for the evaluation of these basic values in digital dentistry. *Int J Comput Dent* 2021;24:341–52.
- Bae E-J, Jeong I-D, Kim W-C, Kim J-H. A comparative study of additive and subtractive manufacturing for dental restorations. *J Prosthet Dent* 2017;118: 187–93. <https://doi.org/10.1016/j.prosdent.2016.11.004>.
- Hickel R, Brühaver K, Ilie N. Repair of restorations – Criteria for decision making and clinical recommendations. *Dent Mater* 2013;29:28–50. <https://doi.org/10.1016/j.dental.2012.07.006>.
- Spijker A, Rodriguez J, Kreulen C, Bronkhorst E, Bartlett D, Creugers N. Prevalence of tooth wear in adults. *Int J Prosthodont* 2009;22:35–42.
- United Nations. Department of Economic and Social Affairs. The Sustainable Development Goals: Report 2022. UN; 2022.
- Duane B, Stancliffe R, Miller F, Sherman J, Pasdeki-Clewer E. Sustainability in dentistry: a multifaceted approach needed. *002203452091939 J Dent Res* 2020;99. <https://doi.org/10.1177/0022034520919391>.
- Duane B., editor. Sustainable Dentistry: Making a Difference. Cham: Springer International Publishing; 2022. <https://doi.org/10.1007/978-3-031-07999-3>.
- Burgelman J-C, Pascu C, Szkuta K, Von Schomberg R, Karalopoulos A, Repanas K, et al. Open science, open data, and open scholarship: european policies to make science fit for the twenty-first century. *Front Big Data* 2019;2:43. <https://doi.org/10.3389/fdata.2019.00043>.
- Govaart GH, Hofmann SM, Medawar E. The sustainability argument for open science. *Collabra Psychol* 2022;8:35903. <https://doi.org/10.1525/collabra.35903>.
- Wuersching SN, Hickel R, Edelhoff D, Kollmuss M. Initial biocompatibility of novel resins for 3D printed fixed dental prostheses. *Dent Mater* 2022;38:1587–97. <https://doi.org/10.1016/j.dental.2022.08.001>.
- Grzebieluch W, Kowalewski P, Grygier D, Rutkowska-Gorczyca M, Kozakiewicz M, Jurczyszyn K. Printable and machineable dental restorative composites for CAD/CAM application—comparison of mechanical properties, fractographic, texture and fractal dimension analysis. *Materials* 2021;14:4919. <https://doi.org/10.3390/ma14174919>.
- Lim BS, Ferracane JL, Condon JR, Adey JD. Effect of filler fraction and filler surface treatment on wear of microfilled composites. *Dent Mater* 2002;18:1–11. [https://doi.org/10.1016/s0109-5641\(00\)00103-2](https://doi.org/10.1016/s0109-5641(00)00103-2).
- Prause E, Malgaj T, Kocjan A, Beuer F, Hey J, Jevnikar P, et al. Mechanical properties of 3D-printed and milled composite resins for definitive restorations: an in vitro comparison of initial strength and fatigue behavior. *J Esthet Restor Dent* 2024;36:391–401. <https://doi.org/10.1111/jerd.13132>.
- Sodeyama MK, Ikeda H, Nagamatsu Y, Masaki C, Hosokawa R, Shimizu H. Printable PICN composite mechanically compatible with human teeth. *J Dent Res* 2021;100:1475–81. <https://doi.org/10.1177/00220345211012930>.
- Lichtenborg J, Willems E, Zhang F, Wesemann C, Weiss F, Nold J, et al. Accuracy of additively manufactured zirconia four-unit fixed dental prostheses fabricated by stereolithography, digital light processing and material jetting compared with subtractive manufacturing. *Dent Mater* 2022;38:1459–69. <https://doi.org/10.1016/j.dental.2022.06.026>.
- Zhao M, Geng Y, Fan S, Yao X, Zhu M, Zhang Y. 3D-printed strong hybrid materials with low shrinkage for dental restoration. *Compos Sci Technol* 2021;213:108902. <https://doi.org/10.1016/j.compscitech.2021.108902>.
- Zhao M, Yang D, Fan S, Yao X, Wang J, Zhu M, et al. 3D-printed strong dental crown with multi-scale ordered architecture, high-precision, and bioactivity. *Adv Sci* 2022;9:2104001. <https://doi.org/10.1002/adv.202104001>.
- Deakin RE, Kildea DG. A note on standard deviation and RMS. *Aust Surv* 1999;44: 74–9. <https://doi.org/10.1080/00050351.1999.10558776>.

- [44] Park J-M, Jeon J, Koak J-Y, Kim S-K, Heo S-J. Dimensional accuracy and surface characteristics of 3D-printed dental casts. *J Prosthet Dent* 2021;126:427–37. <https://doi.org/10.1016/j.prosdent.2020.07.008>.
- [45] Greeff GP, Schilling M. Single print optimisation of fused filament fabrication parameters. *Int J Adv Manuf Technol* 2018;99:845–58. <https://doi.org/10.1007/s00170-018-2518-4>.
- [46] Kaplan D, Rorberg S, Ben Chen M, Sterman Y. NozMod: Nozzle modification for efficient FDM 3d printing. *Proc. 7th Annu. ACM Symp. Comput. Fabr., Seattle WA USA: ACM*. 2022. p. 1–9. <https://doi.org/10.1145/3559400.3561999>.
- [47] Lohbauer U, Belli R, Ferracane JL. Factors involved in mechanical fatigue degradation of dental resin composites. *J Dent Res* 2013;92:584–91. <https://doi.org/10.1177/0022034513490734>.
- [48] Piedra-Cascón W, Krishnamurthy VR, Att W, Revilla-León M. 3D printing parameters, supporting structures, slicing, and post-processing procedures of vat-polymerization additive manufacturing technologies: a narrative review. *J Dent* 2021;109:103630. <https://doi.org/10.1016/j.jdent.2021.103630>.

6. References

- [1] Turkistani A, Nakashima S, Shimada Y, Tagami J, Sadr A. Microgaps and Demineralization Progress around Composite Restorations. *J Dent Res* 2015;94:1070–7. <https://doi.org/10.1177/0022034515589713>.
- [2] Angeletaki F, Gkogkos A, Papazoglou E, Kloukos D. Direct versus indirect inlay/onlay composite restorations in posterior teeth. A systematic review and meta-analysis. *J Dent* 2016;53:12–21. <https://doi.org/10.1016/j.jdent.2016.07.011>.
- [3] Wierichs RJ, Kramer EJ, Meyer-Lueckel H. Risk Factors for Failure of Direct Restorations in General Dental Practices. *J Dent Res* 2020;99:1039–46. <https://doi.org/10.1177/0022034520924390>.
- [4] Boaro LCC, Brandt WC, Meira JBC, Rodrigues FP, Palin WM, Braga RR. Experimental and FE displacement and polymerization stress of bonded restorations as a function of the C-Factor, volume and substrate stiffness. *J Dent* 2014;42:140–8. <https://doi.org/10.1016/j.jdent.2013.11.016>.
- [5] Rodrigues FP, Silikas N, Watts DC, Ballester RY. Finite element analysis of bonded model Class I ‘restorations’ after shrinkage. *Dent Mater* 2012;28:123–32. <https://doi.org/10.1016/j.dental.2011.10.001>.
- [6] Kowalczyk P. Influence of the shape of the layers in photo-cured dental restorations on the shrinkage stress peaks—FEM study. *Dent Mater* 2009;25:e83–91. <https://doi.org/10.1016/j.dental.2009.07.014>.
- [7] Li H, Li J, Zou Z, Fok AS-L. Fracture simulation of restored teeth using a continuum damage mechanics failure model. *Dent Mater* 2011;27:e125–33. <https://doi.org/10.1016/j.dental.2011.03.006>.
- [8] Ichim I, Li Q, Loughran J, Swain M, Kieser J. Restoration of non-cariou cervical lesions Part I. Modelling of restorative fracture. *Dent Mater* 2007;23:1553–61. <https://doi.org/10.1016/j.dental.2007.02.003>.
- [9] Nandini S. Indirect resin composites. *J Conserv Dent* 2010;13:184–94. <https://doi.org/10.4103/0972-0707.73377>.
- [10] Daher R, Ardu S, di Bella E, Krejci I, Duc O. Efficiency of 3D printed composite resin restorations compared with subtractive materials: Evaluation of fatigue behavior, cost, and time of production. *J Prosthet Dent* 2024;131:943–50. <https://doi.org/10.1016/j.prosdent.2022.08.001>.
- [11] Al Hamad KQ, Al Rashdan RB, Al Rashdan BA, Al Quran FA. Effect of CAD-CAM tool deterioration on the trueness of ceramic restorations. *J Prosthet Dent* 2022;127:635–44. <https://doi.org/10.1016/j.prosdent.2020.09.035>.
- [12] Ausiello P, Ciaramella S, Di Rienzo A, Lanzotti A, Ventre M, Watts DC. Adhesive class I restorations in sound molar teeth incorporating combined resin-composite and glass ionomer materials: CAD-FE modeling and analysis. *Dent Mater* 2019;35:1514–22. <https://doi.org/10.1016/j.dental.2019.07.017>.
- [13] Kaisarly D, El Gezawi M, Xu X, Rösch P, Kunzelmann K-H. Shrinkage vectors of a flowable composite in artificial cavity models with different boundary conditions: Ceramic and Teflon. *J Mech Behav Biomed Mater* 2018;77:414–21. <https://doi.org/10.1016/j.jmbbm.2017.10.004>.

-
- [14] Novaes JB, Talma E, Las Casas EB, Aregawi W, Kolstad LW, Mantell S, et al. Can pulpal floor debonding be detected from occlusal surface displacement in composite restorations? *Dent Mater* 2018;34:161–9. <https://doi.org/10.1016/j.dental.2017.11.019>.
- [15] Wang Z, Chiang MYM. Correlation between polymerization shrinkage stress and C-factor depends upon cavity compliance. *Dent Mater* 2016;32:343–52. <https://doi.org/10.1016/j.dental.2015.11.003>.
- [16] Feilzer AJ, De Gee AJ, Davidson CL. Setting Stress in Composite Resin in Relation to Configuration of the Restoration. *J Dent Res* 1987;66:1636–9. <https://doi.org/10.1177/00220345870660110601>.
- [17] Liu X, Li H, Li J, Lu P, Fok AS-L. An acoustic emission study on interfacial debonding in composite restorations. *Dent Mater* 2011;27:934–41. <https://doi.org/10.1016/j.dental.2011.05.008>.
- [18] Watts DC, Satterthwaite JD. Axial shrinkage-stress depends upon both C-factor and composite mass. *Dent Mater* 2008;24:1–8. <https://doi.org/10.1016/j.dental.2007.08.007>.
- [19] Aregawi WA, Fok ASL. Shrinkage stress and cuspal deflection in MOD restorations: analytical solutions and design guidelines. *Dent Mater* 2021;37:783–95. <https://doi.org/10.1016/j.dental.2021.02.003>.
- [20] Oginni AO, Adeleke AA. Comparison of pattern of failure of resin composite restorations in non-carious cervical lesions with and without occlusal wear facets. *J Dent* 2014;42:824–30. <https://doi.org/10.1016/j.jdent.2014.04.003>.
- [21] Rees JS, Jacobsen PH. The effect of cuspal flexure on a buccal Class V restoration: a finite element study. *J Dent* 1998;26:361–7. [https://doi.org/10.1016/S0300-5712\(97\)00015-8](https://doi.org/10.1016/S0300-5712(97)00015-8).
- [22] Soares P, Machado A, Zeola L, Souza P, Galvão A, Montes T, et al. Loading and composite restoration assessment of various non-carious cervical lesions morphologies – 3D finite element analysis. *Aust Dent J* 2015;60:309–16. <https://doi.org/10.1111/adj.12233>.
- [23] Hong H-H, Liu H-L, Hong A, Chao P. Inconsistency in the Crown-to-Root Ratios of Single-Rooted Premolars Measured by 2D and 3D Examinations. *Sci Rep* 2017;7:16484. <https://doi.org/10.1038/s41598-017-16612-x>.
- [24] Ribes A, Caremoli C. Salomé platform component model for numerical simulation. 31st Annu. Int. Comput. Softw. Appl. Conf. COMPSAC 2007, vol. 2, 2007, p. 553–64. <https://doi.org/10.1109/COMPSAC.2007.185>.
- [25] Électricité de France. Finite element code_aster, Analysis of Structures and Thermomechanics for Studies and Research 2021.
- [26] Lüchtenborg J, Willems E, Zhang F, Wesemann C, Weiss F, Nold J, et al. Accuracy of additively manufactured zirconia four-unit fixed dental prostheses fabricated by stereolithography, digital light processing and material jetting compared with subtractive manufacturing. *Dent Mater* 2022;38:1459–69. <https://doi.org/10.1016/j.dental.2022.06.026>.
- [27] Grzebieluch W, Kowalewski P, Grygier D, Rutkowska-Gorczyca M, Kozakiewicz M, Jurczyszyn K. Printable and Machinable Dental Restorative Composites for CAD/CAM Application—Comparison of Mechanical Properties, Fractographic, Texture and Fractal Dimension Analysis. *Materials* 2021;14:4919. <https://doi.org/10.3390/ma14174919>.

-
- [28] Lin C-H, Lin Y-M, Lai Y-L, Lee S-Y. Mechanical properties, accuracy, and cytotoxicity of UV-polymerized 3D printing resins composed of Bis-EMA, UDMA, and TEGDMA. *J Prosthet Dent* 2020;123:349–54. <https://doi.org/10.1016/j.prosdent.2019.05.002>.
- [29] Lim BS, Ferracane JL, Condon JR, Adey JD. Effect of filler fraction and filler surface treatment on wear of microfilled composites. *Dent Mater* 2002;18:1–11. [https://doi.org/10.1016/s0109-5641\(00\)00103-2](https://doi.org/10.1016/s0109-5641(00)00103-2).
- [30] Prause E, Malgaj T, Kocjan A, Beuer F, Hey J, Jevnikar P, et al. Mechanical properties of 3D-printed and milled composite resins for definitive restorations: An in vitro comparison of initial strength and fatigue behavior. *J Esthet Restor Dent* 2024;36:391–401. <https://doi.org/10.1111/jerd.13132>.
- [31] Saadi MASR, Maguire A, Pottackal NT, Thakur MSH, Ikram MMd, Hart AJ, et al. Direct Ink Writing: A 3D Printing Technology for Diverse Materials. *Adv Mater* 2022;34:2108855. <https://doi.org/10.1002/adma.202108855>.
- [32] Farahani RD, Lebel LL, Therriault D. Processing parameters investigation for the fabrication of self-supported and freeform polymeric microstructures using ultra-violet-assisted three-dimensional printing. *J Micromechanics Microengineering* 2014;24:055020. <https://doi.org/10.1088/0960-1317/24/5/055020>.
- [33] Wang T-M, Lee M-S, Knezevic A, Tarle Z, Chiang Y-C, Kunzelmann K-H. Evaluation of the slumping property of dental composites during modeling. *J Dent Sci* 2012;7:330–5. <https://doi.org/10.1016/j.jds.2012.04.002>.
- [34] Greeff GP, Schilling M. Single print optimisation of fused filament fabrication parameters. *Int J Adv Manuf Technol* 2018;99:845–58. <https://doi.org/10.1007/s00170-018-2518-4>.

Curriculum vitae

Po-Chun Tseng

B97502092@ntu.edu.tw | ORCID [0000-0002-1592-0905](https://orcid.org/0000-0002-1592-0905)

EDUCATION

PhD Candidate in Oral Sciences, Ludwig Maximilian University of Munich *Apr. 2021 – 2025*

- Research focus: novel 3D printing technologies and numerical simulation in dentistry (Advisors: [Prof. Dr. Karl-Heinz Kunzelmann](#) ✉, PD. Dr. Andreas Kessler, Prof. Dr. Peter Rösch, PD. Dr. Dalia Kaisarly)
- Relevant Coursework: Machine Learning for Engineers I & II, Artificial Intelligence and Global Health, Academic Writing, Entrepreneurial Skills, Academic Entrepreneurship

Master of Science in Dental Materials, National Cheng Kung University, Taiwan *2016 – 2019*

- Specialty training in conservative dentistry
- Research-oriented coursework: Engineering mathematics, Biopolymer Science, Biophysics, Biomechanics, Physical Chemistry, Digital Image Processing, Electron Microscopy, Biostatistics
- GPA: 4.17/4.3, Phi Tau Phi Scholastic Honor

Doctor of Dental Surgery, National Taiwan University, Taiwan *2008 – 2015*

- Externship at University of Pennsylvania and National University of Singapore

PROFESSIONAL EXPERIENCE

PhD Module in Biomedical Engineering, EIT Health, European Union *Jun. 2023 – Present*

- Selected for EU-funded multidisciplinary program for R&D skills and entrepreneurship training
- Ongoing collaborations with Universidad Politécnica de Madrid

Certified Carpentries Instructor, The Carpentries Organization *Apr. 2024*

- Trained for live coding based on the evidence-based teaching practices (the science of learning)
- Co-instructed an on-site live coding workshop (R visualization) as a LMU Open Science Fellow

AI Safety Fundamentals: Alignment Challenge, Effective Altruism Germany *Winter 2023*

- Hybrid projects and in-depth discussions about the BlueDot Impact curriculum

International Summer School on AI Applications in Medicine, TU Dresden, Germany *Sep. 2023*

- Well acquainted with cutting-edge development of AI in the medical context

CED-IADR Summer School, Uni Regensburg, Germany *Jun. 2023*

- Profound understanding of advanced dental material analysis

Coding Bootcamp, 42 Heilbronn, Germany *Feb. 2022*

- Intensive project-based self-learning for C programming

Research Internship, Max Planck Institute of Biochemistry, Germany *Jul. 2018 – Aug. 2018*

- Research project: Micro-biofabrication with two-photon stereolithography

HONORS

Academy of Dental Materials Paffenbarger Award (2024, first prize among 41 applicants worldwide)

International Association for Dental Research Continental European Division (CED-IADR) Travel Grant (2024)

Dental Innovation Award, Stiftung Innovative Zahnmedizin (2023)

DGR²Z-Kulzer-Start Research Grant (2023)

IADR Kulzer Travel Award (2023)

Oral Presentation Award, Asian-Oceanian Federation of Conservative Dentistry (2023)

Paffenbarger Award finalist, Academy of Dental Materials (2022, top 6 among 28 applicants)

Best Research Award, Taiwan Academy of Operative Dentistry General Session (2020)

Invited speaker, National Synchrotron Radiation Research Center (NSRRC) Users' Meeting (2019)

First-Prize, IADR-SEA Unilever Hatton Divisional Award-Senior Category (2018)

Student Research Award, Nanosystems Initiative Munich (2018)

Merit Award, National Cheng Kung University Institute of Oral Medicine (2017)

PUBLICATIONS

Tseng PC, Shieh DB, Kessler A, Kaisarly D, Rösch P, Kunzelmann KH. Direct ink writing with dental composites: A paradigm shift toward sustainable chair-side production. *Dental Materials* 2024;40:1753–61. <https://doi.org/10.1016/j.dental.2024.08.002>.

Benz L, Heck K, Hevisov D, Kugelmann D, **Tseng PC**, Sreij Z, Litzemberger F, Waschke J, Schwendicke F, Kienle A, Hickel R, Kunzelmann K-H, Walter E, Visualization of Pulpal Structures by SWIR in Endodontic Access Preparation. *Journal of Dental Research* 2024;103:1375–83. <https://doi.org/10.1177/00220345241262949>.

Tseng PC, Chuang SF, Schulz-Kornas E, Kunzelmann KH, Kessler A. Elucidating interfacial failure of cervical restorations using damage mechanics: A finite element analysis. *Journal of Dental Sciences* 2025;20:410–6. <https://doi.org/10.1016/j.jds.2024.05.033>.

Tseng PC, Chuang SF, Kaisarly D, Kunzelmann KH. Simulating the shrinkage-induced interfacial damage around Class I composite resin restorations with damage mechanics. *Dental Materials* 2023;39:513–21. <https://doi.org/10.1016/j.dental.2023.03.020>.

Tseng PC, Lee CL, Chuang SF. "Cast gold partial-coverage restoration for patients with heavy occlusal load: a case report", *J Taiwan Acad Oper Dent* 2020;10.1: 66–74.

SKILLS

Programming: Python, R, C, C#, Matlab

Microscopy and Spectroscopy: SEM, FTIR, CLSM, Optical Coherence Tomography

Image Processing and In-silico Biomechanics: ImageJ, 3D Slicer, CloudCompare, Salome-MECA

Acknowledgements

I would like to express sincere gratitude to all who supported me during this scientific expedition.

First of all, I am more than grateful to Prof. Dr. Karl-Heinz Kunzelmann for his unwavering support. His vision has been inspiring me well before the beginning of the PhD program. I am extremely fortunate to be mentored by a distinguished clinician-scientist with a unique combination of technical expertise, theoretical knowledge, and philosophical thinking. Thank you, Prof. Kunzelmann, for your guidance over the past four years.

Special thanks to all the members of my supervision committee. I learned how to conduct research and collaborate with others from their feedback. I especially appreciate PD. Dr. Andreas Kessler's openness and Prof. Peter Rösch's scientific rigor. This mentorship unequivocally lays an invaluable foundation for my scientific exploration.

I would like to express special thanks to Mr. Thomas Obermeier and Mr. Georg Hiebl for providing technical support and inspiration, and to Ms. Gisela Dachs and Ms. Eva Köbele for their efforts. Their dedication contributed to the progress of material science in dentistry.

Furthermore, I broadened my perspectives through the research projects with PD. Dr. Katrin Heck, Dr. Elias Walter, Dr. Raphaël Richert, and Dr. Ellen Schulz-Kornas. I genuinely appreciate the friendships and collaborations developed during my stay in Europe. Also, I am grateful to have the opportunity to keep learning from my master's supervisors, Prof. Dar-Bin Shieh and Prof. Shu-Fen Chuang. I will stay connected and contribute together to positive impacts in the future.

I gratefully acknowledge the scholarship funding from DAAD (German Academic Exchange Service), the GSSA scholarship from the Ministry of Education Taiwan, and the visiting scholar grant from Forschungsgemeinschaft Dental e.V.

Finally, my utmost gratitude to my beloved wife, my sister, and my parents for all the support. I am especially grateful to have Pei-Hsuan accompany me for the past many years, and this extended journey would not have been possible without the understanding of all of you.